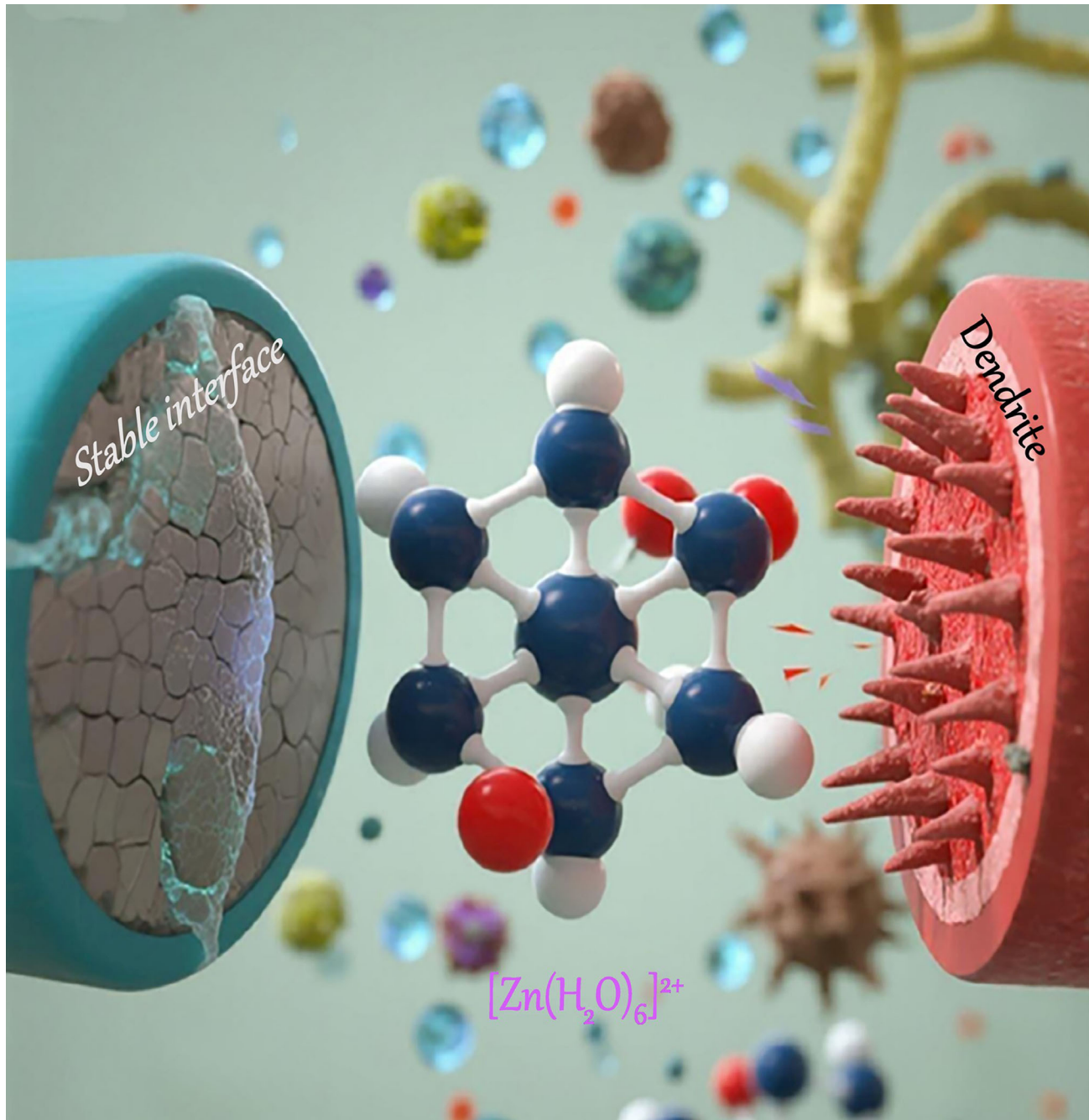


Electrolyte Additives for Enhanced Aqueous Zinc-Ion Battery Performance

Junxiang Liu, Zhihong Peng, Ruanming Liao, Junli Zhou,* and Qianyu Zhang*



Aqueous zinc-ion batteries (AZIBs) have emerged as a promising next-generation energy storage technology due to their superior safety, low cost, and high volumetric capacity, particularly in the context of large-scale energy storage. Despite these advantages, ZIBs still face several practical challenges, such as zinc dendrite growth, hydrogen evolution reaction (HER), and zinc anode corrosion, which significantly impact their Coulombic efficiency, reversibility, and cycle life, thereby limiting their widespread adoption. In recent years, researchers have proposed various

electrolyte additives to address these issues. This article systematically reviews the application of electrolyte additives in AZIBs, focusing on how different types of additives can effectively mitigate these challenges by modulating the Zn^{2+} solvation structure, forming protective layers at the anode–electrolyte interface, balancing Zn^{2+} distribution, and promoting uniform zinc deposition. Finally, potential research directions and future prospects for improving and guiding the development of electrolyte additives for AZIBs are discussed.

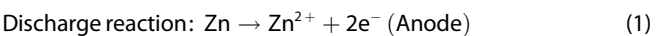
1. Introduction

With the growing global demand for clean energy—particularly in sectors such as electric vehicles (EVs) and renewable energy storage—innovation in battery technologies has become a crucial driver of the energy transition.^[1] Currently, lithium-ion batteries (Li-ion batteries) remain the most widely used energy storage systems. However, their high cost, reliance on limited resources (such as lithium and cobalt), and potential safety hazards associated with organic electrolytes have prompted researchers to seek safer, more cost-effective, and sustainable alternatives.^[2–4] As a result, sodium-ion batteries (SIBs) and potassium-ion batteries have attracted considerable attention due to the abundance and low cost of sodium and potassium. Nevertheless, their widespread use of organic electrolytes introduces significant safety concerns, including high flammability and poor thermal stability, which limit their applicability in high-temperature and high-power environments.^[5,6] Multivalent ion systems, such as magnesium-ion and calcium-ion batteries, offer promising theoretical capacities and volumetric energy densities, but remain in the early stages of development. Their progress is hindered by sluggish ion transport, poor electrode compatibility, and interfacial instability.^[7] Among emerging battery technologies, zinc-ion batteries (ZIBs) have garnered increasing attention owing to their advantages in resource availability, safety, and environmental friendliness.^[8,9] Zinc features a high theoretical capacity, moderate redox potential, good reversibility, and low cost, making it an attractive candidate for constructing high-performance

rechargeable batteries.^[10–12] In particular, aqueous ZIBs (AZIBs), which employ water-based electrolytes, exhibit inherent benefits such as nonflammability, high ionic conductivity, and environmental compatibility. These characteristics confer significant advantages over conventional battery systems in terms of safety and sustainability.^[13–15] Taken together, these features make AZIBs a highly promising alternative to overcome the limitations of current battery technologies.

As a typical class of rechargeable secondary batteries, AZIBs consist of a series of functional components, including a cathode material, an anode material, an electrolyte, a separator, and a current collector (Figure 1a).^[16,17] Zinc metal is widely employed as the anode due to its high theoretical capacity (820 mAh g^{-1}), low electrode potential (-0.76 V vs. Standard Hydrogen Electrode), and low cost.^[18] The electrolyte typically consists of neutral or mildly acidic aqueous solutions of zinc salts, such as ZnSO_4 and $\text{Zn}(\text{CF}_3\text{SO}_3)_2$. These electrolytes not only exhibit good ionic conductivity but also offer high safety and environmental friendliness.^[19] Regarding cathode materials, extensive research has been conducted on manganese-based compounds,^[20,21] vanadium-based compounds,^[22,23] Prussian blue analogs,^[24,25] and organic materials.^[26,27] These cathode materials can reversibly insert and extract Zn^{2+} during the charge/discharge process, which is essential for achieving high capacity and excellent cycling stability. AZIBs share a similar electrochemical working mechanism with LIBs, in which energy storage and release rely on the reversible migration of charge carriers between the anode and cathode (Figure 1b).^[28] Specifically, the energy storage mechanisms of AZIBs mainly include three types: 1) reversible Zn^{2+} intercalation/deintercalation into/from the electrode materials;^[29] 2) coinsertion reactions involving both Zn^{2+} and H^+ ions;^[30] and 3) conversion-type reactions based on chemical transformation of the electrode materials.^[31] These mechanisms collectively ensure the efficient transport and stable storage of zinc ions during the cycling process.

During the charge and discharge processes, Zn^{2+} ions migrate through the electrolyte—being released from the anode during charging and reinserted into the cathode material during discharging. This intercalation/deintercalation process constitutes the core energy storage mechanism of AZIBs.^[32] The corresponding electrochemical reactions can be represented as follows.



J. Liu, Z. Peng, R. Liao, J. Zhou
Key Laboratory of Clean Chemistry Technology of Guangdong Regular Higher Education Institution
School of Chemical Engineering and Light Industry
Guangdong University of Technology
Guangzhou 510006, China
E-mail: zhouljees@gdut.edu.cn

J. Zhou
Guangdong Provincial Laboratory of Chemistry and Fine Chemical Engineering Jieyang Center
Jieyang 515200, China

Q. Zhang
College of Materials Science and Engineering
Sichuan University
Chengdu 610064, China
E-mail: zhangqianyu@scu.edu.cn

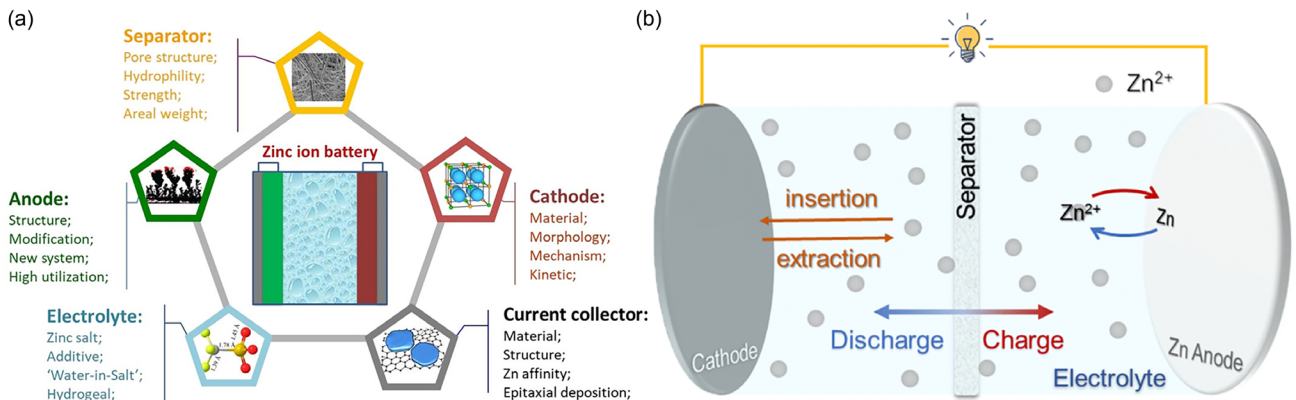
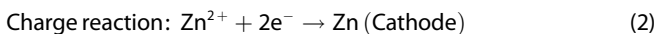


Figure 1. a) Structural components of AZIB. Reproduced with permission.^[17] Copyright (2020), Wiley-VCH. b) Schematic illustration of the working mechanism of AZIB. Reproduced under the terms of the CC-BY Creative Commons Attribution 3.0 Unported License.^[28] Copyright 2023, X. Guo and G. He, Published by the Royal Society of Chemistry.



Through this ion intercalation/deintercalation-based energy storage mechanism, AZIBs exhibit favorable cycling stability and low environmental risk.

Despite the significant advantages of AZIBs in terms of safety and cost, several technical challenges remain. First, the electrochemical stability window (ESW) of aqueous electrolytes is relatively narrow (≈ 1.23 V), which limits the application of high-voltage cathode materials and thereby constrains the overall energy density of the battery.^[33] In addition, zinc tends to deposit unevenly on the anode surface during cycling, leading to the formation of zinc dendrites. This not only degrades the cycling performance of the battery but may also cause short circuits and even battery failure.^[34] Therefore, enhancing the stability of aqueous electrolytes and expanding their ESW have become key strategies for improving the performance of AZIBs.^[28]

To address these challenges, researchers have recently explored the use of electrolyte additives to optimize electrolyte performance and thereby enhance the overall performance of

AZIBs.^[19,35,36] Electrolyte additives include inorganic salts, organic compounds, polymeric materials, and emerging ionic liquids (ILs). These additives serve various functions, such as regulating the pH of the electrolyte, forming stable interfacial layers on electrodes, promoting uniform zinc deposition, expanding the ESW, and suppressing undesirable side reactions.^[19,37,38] For instance, certain polymer additives such as gelatin and polyvinylpyrrolidone (PVP) can adsorb onto the zinc surface, facilitating uniform zinc plating and effectively inhibiting dendrite formation.^[39–41] Small organic molecules like acetic acid and ethylenediaminetetraacetic acid (EDTA) can chelate Zn^{2+} ions, modulate their concentration distribution at the electrode interface, and consequently improve the cycling performance and stability of the battery.^[42,43] Moreover, the incorporation of ILs and specific organic additives has been demonstrated to significantly broaden the ESW, enhancing the operational stability of AZIBs under high-voltage conditions.^[43–46] As a result, the development of electrolyte additives has become a critical direction in advancing AZIB technology. Through rational design and careful selection of additives, it is possible not only to improve the conductivity and stability of



Junxiang Liu is currently pursuing his master's degree at the School of Light Industry and Chemical Engineering, Guangdong University of Technology, Guangzhou, China, under the supervision of Associate Professor Junli Zhou. His research focuses on rechargeable batteries and hydrogen production via water electrolysis.



Junli Zhou, Ph.D., is an associate professor and master's supervisor at Guangdong University of Technology. Her research mainly focuses on new energy materials and energy storage devices, including novel catalytic materials, supercapacitors, and lithium-ion batteries. She has published dozens of SCI-indexed papers and holds several authorized patents.



Qianyu Zhang, Ph.D., is an associate professor and doctoral advisor at Sichuan University. His research focuses on aqueous batteries, solid-state batteries, lithium-sulfur, and alkali-ion batteries. He has published 60+ SCI papers (2 ESI Highly Cited, 1 Hot Paper) in top journals like EES, JACS, AM, and Angew Chem, with 2400+ citations and H-index of 28. He leads multiple national and provincial projects and serves as a reviewer and editorial board member for several journals.

electrolytes but also to suppress parasitic reactions, thereby increasing battery safety and extending cycle life.

This review focuses on recent progress in electrolyte additives for AZIBs, highlighting their classification, functional mechanisms, and performance impacts and further providing perspectives on future research trends.

2. Classification of Electrolyte Additives for Aqueous ZIBs

The development pathway of electrolyte additives for AZIBs is illustrated in Figure 2. As shown in Figure 3, these additives can be broadly classified into four main categories: organic additives, inorganic additives, IL additives, and composite additives. Through various mechanisms—such as modulating the solvation structure, optimizing interfacial electrochemical reactions, and suppressing side reactions (e.g., hydrogen evolution and dendrite formation)—these additives have been shown to significantly improve the cycling stability, Coulombic efficiency, and energy density of AZIBs.^[8,19,28,37] In recent years, with the rapid advancement of in situ characterization techniques and theoretical computational methods, the understanding of additive mechanisms has gradually evolved from macroscopic phenomenological descriptions to atomistic-level dynamic insights. This transition provides a new perspective and theoretical foundation for the rational design and application of high-performance additives.^[37,47–49]

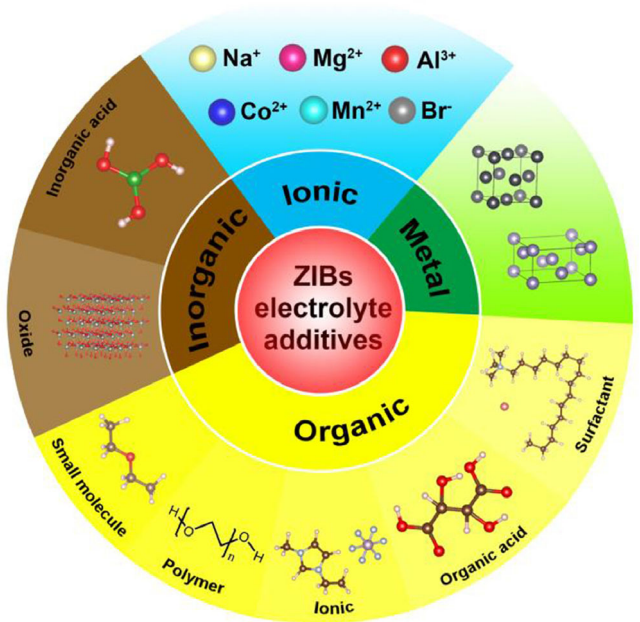


Figure 3. Overview of the classification of electrolyte additives for AZIBs.^[50] Reprinted from Energy Storage Materials, Vol. 34, Shan Guo, Liping Qin, Tengsheng Zhang, Miao Zhou, Jiang Zhou, Guozhao Fang, Shuquan Liang, "Fundamentals and perspectives of electrolyte additives for aqueous zinc-ion batteries," Pages 545–562, Copyright (2020), with permission from Elsevier.

Therefore, this article provides a comprehensive classification of electrolyte additives used in AZIBs and systematically discusses their roles and mechanisms in enhancing battery performance.

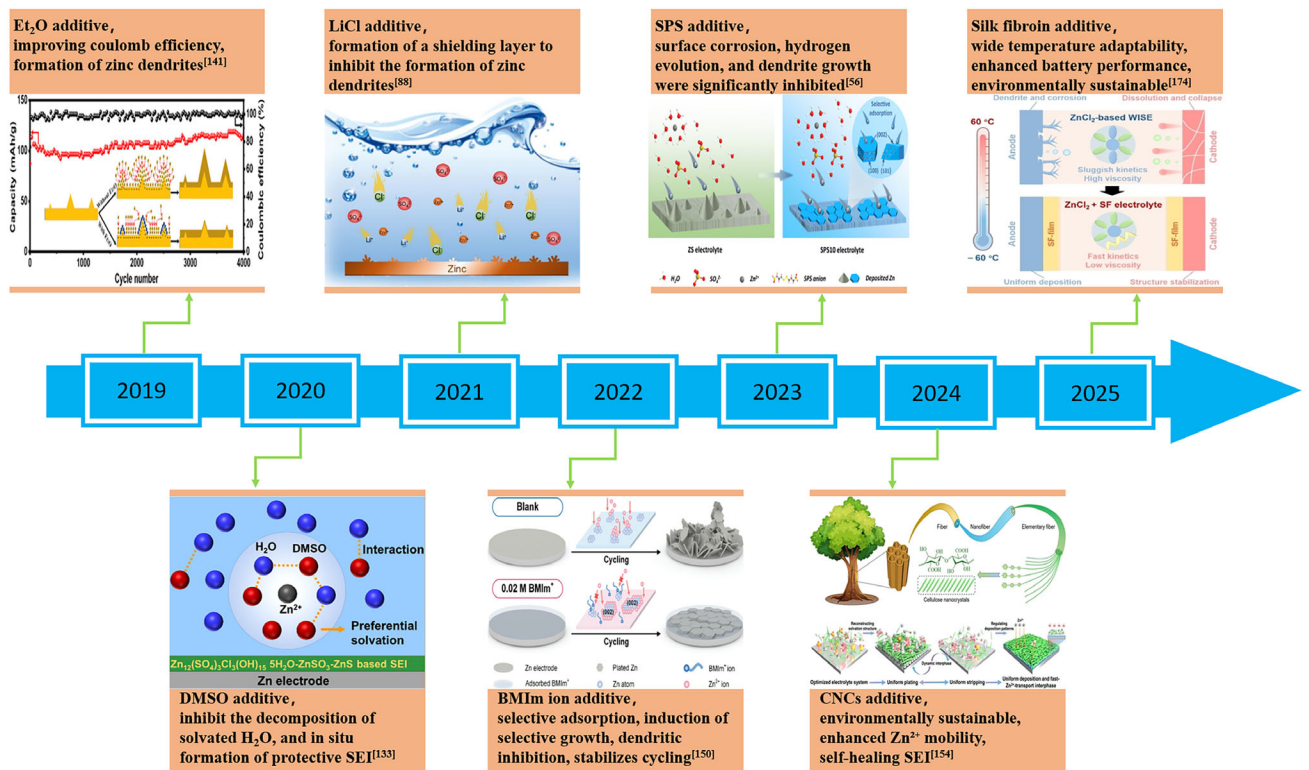


Figure 2. Development process of electrolyte additives for AZIBs.

2.1. Organic Additives

As an important class of materials in AZIBs, organic additives play a vital role in enhancing battery performance through multiple mechanisms. They can significantly improve the electrochemical behavior of AZIBs by regulating the ionic conductivity of the electrolyte, suppressing zinc dendrite growth, stabilizing the electrode–electrolyte interface, and extending cycling life.^[43,51,52] In recent years, with continuous advancements in synthetic chemistry and battery technologies, the design and application of organic additives have become increasingly diverse, making them a key strategy for optimizing the performance of AZIBs.

2.1.1. Surfactant-Type Additives

Surfactants are amphiphilic organic molecules widely used in AZIBs to regulate interfacial behavior at the zinc anode.^[43] By forming an adsorbed layer on the zinc surface, they reduce surface energy and induce uniform Zn^{2+} deposition, thereby suppressing dendrite growth and parasitic reactions (such as hydrogen evolution), ultimately improving the cycling stability and Coulombic efficiency of the battery.^[50] Based on the dissociation properties of their polar head groups, surfactants can be classified into four categories: cationic, anionic, zwitterionic, and nonionic.

Cationic surfactants such as tetramethylammonium sulfate hydrate (TMA_2SO_4) and benzyltrimethylammonium (TMBAC) have shown excellent interfacial regulation capabilities in AZIBs. Cao et al.^[53] reported a low-cost, efficient, and nontoxic electrolyte additive— TMA_2SO_4 —as a cationic surfactant that can effectively promote uniform zinc deposition during cycling. Remarkably, even at a low concentration of 0.25 mM, TMA_2SO_4 guided lateral Zn^{2+} deposition along the zinc foil surface rather than vertical growth (Figure 4a–f), significantly suppressing dendrite formation and side reactions. At a current density of 0.5 mA cm^{-2} and areal capacity of 0.5 mAh cm^{-2} , the Zn–Zn symmetric cell with TMA_2SO_4 achieved over 1800 h of stable cycling, demonstrating outstanding longevity. Furthermore, when paired with a MnO_2 cathode, the $Zn||MnO_2$ full cell delivered an initial capacity of 181.3 mAh g^{-1} at 0.2 A g^{-1} , with a capacity retention of 98.72% after 200 cycles. This study introduced the concept of electrostatic shielding as a general strategy for electrolyte design to effectively inhibit zinc dendrite growth and parasitic reactions, offering a new pathway toward highly stable AZIBs. In another study, Guan et al.^[54] systematically investigated the interfacial behavior of three quaternary ammonium cationic surfactants—benzyldimethyldecylammonium chloride (DDBAC, $DDBA^+$ cation), dodecyltrimethylammonium chloride (DTAC, DTA^+ cation), and benzyltrimethylammonium chloride (TMBAC, $TMBA^+$ cation) in $ZnSO_4$ electrolytes. These surfactants share the same hydrophilic quaternary ammonium headgroup but differ in their hydrophobic moieties. Among them, TMBAC (with a benzyl hydrophobic group) exhibited superior performance in promoting uniform Zn deposition and suppressing dendrite growth. Density functional theory (DFT) simulations revealed that $TMBA^+$ cations (from TMBAC) preferentially adsorb onto the

Zn anode surface, forming a compact and ordered monolayer through electrostatic attraction and hydrophobic interaction. This monolayer constructs a hydrophobic Helmholtz region that acts as a barrier against water penetration, thereby significantly inhibiting hydrogen evolution reaction (HER) and formation of $Zn_4(OH)_6SO_4 \cdot xH_2O$ (ZHS) by-products. Furthermore, DFT-calculated energy profiles demonstrated that the diffusion energy barrier for Zn^{2+} migration across the $TMBA^+$ interface is modulated by the spatial arrangement of the cations. The hydrophobic benzyl groups create multichannel structures that guide Zn^{2+} diffusion in a dispersed manner, reducing local current density and dendrite nucleation probability. As a result, TMBAC achieves nearly 100% Coulombic efficiency, minimal polarization hysteresis, and excellent cycle stability. A $Zn-VO_2$ flexible battery with 0.5 g L^{-1} TMBAC electrolyte delivered a high specific capacity of 290 mAh g^{-1} and remained stable over 400 cycles at 5 A g^{-1} without noticeable gas generation (Figure 4g), confirming its ability to suppress side reactions and corrosion through effective interfacial regulation.

Anionic surfactants, such as sodium dodecylbenzenesulfonate (SDBS) and sodium 3,3'-dithiodipropane sulfonate (SPS), have been demonstrated to effectively suppress zinc dendrite growth and mitigate anode corrosion, thereby enhancing the interfacial stability and cycling lifespan of Zn anodes. Lin et al.^[55] employed SPS, a novel anionic surfactant additive, to modulate Zn deposition in aqueous $ZnSO_4$ electrolytes. Unlike conventional additives that alter Zn^{2+} solvation, SPS exhibits negligible impact on the solvation structure, instead regulating deposition through preferential surface adsorption. DFT calculations revealed that SPS anions strongly adsorb onto the Zn (100) and (101) crystal planes, with high adsorption energies (E_{ads}) of -7.35 and -7.16 eV , respectively, while displaying the weakest adsorption on the (002) plane ($E_{ads} = -6.43\text{ eV}$). This selective binding suppresses Zn growth on non-(002) facets, thereby exposing and promoting horizontal growth along the corrosion-resistant (002) orientation. Additionally, the (002) facet exhibited minimal atomic rearrangement upon SPS adsorption, confirming its structural stability and low surface energy. In situ electrochemical atomic force microscopy and optical microscopy directly visualized this behavior (Figure 5a–c): without SPS, Zn deposition proceeded vertically with dendritic protrusions and fiber entanglement (Figure 5d,f), whereas SPS induced a smooth, dense, and horizontally aligned Zn coating (Figure 5e,g). These interfacial modifications significantly improved electrochemical performance. A $Zn || Zn$ soft-pack symmetric cell ($3 \times 5\text{ cm}^2$) using 10 mM SPS electrolyte sustained stable cycling for over 800 h and delivered a cumulative capacity exceeding $12,000\text{ mA h}$. These findings confirm that the interfacial regulation enabled by facet-selective SPS adsorption effectively suppresses dendrite growth, hydrogen evolution, and byproduct accumulation.

In addition, zwitterionic surfactants, which possess both cationic and anionic functional groups, exhibit pH-responsive interfacial behavior. In AZIBs, these additives can spontaneously assemble at the electrode–electrolyte interface to form a compact adsorption layer, which regulates Zn^{2+} nucleation and deposition through charge redistribution and steric hindrance, thereby

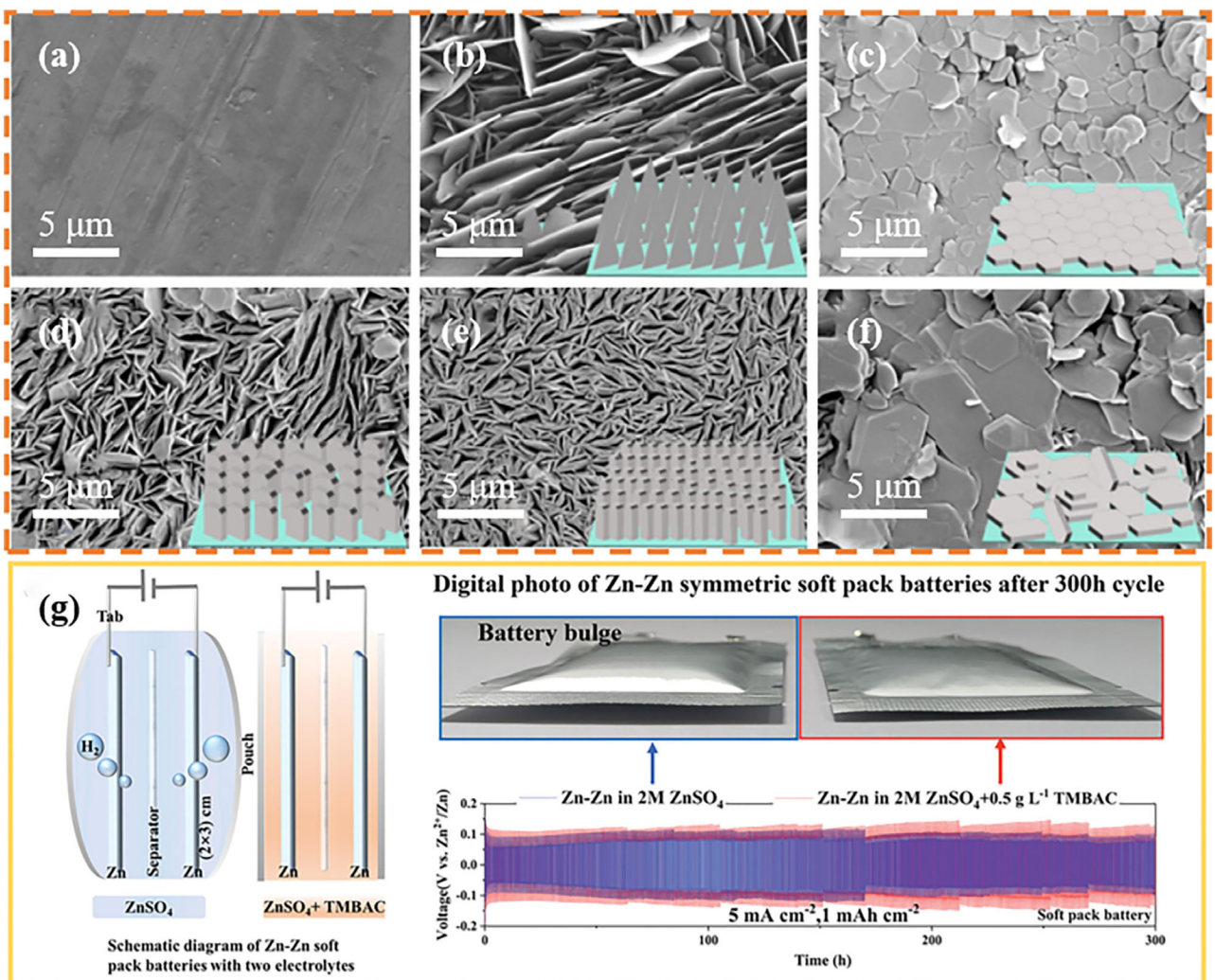


Figure 4. a) SEM image of bare Zn foil without cycling. SEM images of Zn electrode cycled for 100 h in ZnSO_4 (2 M): b) without additive, c) with TMA_2SO_4 , d) with TMAAC, e) with TMCl, and f) with TMANO₃.^[53] Reprinted from Journal of Colloid and Interface Science, Vol. 627, Heng Cao, Xiaomin Huang, Yu Liu, Qiang Hu, Qiaoji Zheng, Yu Huo, Fengyu Xie, Jingxin Zhao, Dunmin Lin, "An efficient electrolyte additive of tetramethylammonium sulfate hydrate for dendrite-free zinc anode for aqueous zinc-ion batteries," Pages 367–374, Copyright (2022), with permission from Elsevier. g) Galvanostatic Zn plating/stripping in Zn-Zn soft pack batteries in two electrolytes.^[54] Copyright (2022), Wiley-VCH. SEM, scanning electron microscopy.

suppressing dendrite formation and side reactions such as hydrogen evolution. Tao et al.^[56] proposed a dual-function interfacial engineering strategy based on the zwitterionic surfactant N-decyl-N,N-dimethyl-3-ammonio-1-propanesulfonate (Z10). Z10 self-assembles into a hydrophobic protective layer on the Zn surface and forms a polarized interfacial layer with an internal electric field, enabling synergistic modulation of interfacial behavior. To investigate the effect of alkyl chain length, structurally analogous derivatives—N-octyl (Z8) and N-tetradecyl (Z14)—were also studied. Experimental and computational results indicated that the moderate electric field induced by Z10 alleviates the “tip effect” and promotes uniform Zn^{2+} migration and deposition, while the hydrophobic layer effectively prevents water molecules from entering the inner Helmholtz plane, thereby suppressing byproduct formation such as ZHS. Under the combined effect of electric field modulation and hydrophobic protection, Z10 significantly improved the cycling stability of Zn anodes, achieving a

prolonged cycle life of up to 2000 h and a high Coulombic efficiency of 99.4% (Figure 5h,i). Furthermore, the AZIB system has also seen research exploring naturally derived or modified zwitterionic surfactants, such as peptone and betaine.^[57,58] These materials exhibit tunable interfacial activity, electrochemical stability, and excellent environmental friendliness, which help mitigate side reactions and enhance battery performance. As such, they offer a promising direction for the development of greener and more sustainable electrolyte systems.

Nonionic surfactants, due to the absence of ionizable functional groups, exhibit surface activity primarily through the synergistic interaction between their hydrophilic and hydrophobic molecular segments.^[59] These surfactants demonstrate superior tolerance to variations in ionic strength and pH compared to conventional ionic surfactants, whose performance often deteriorates under high salt concentrations or fluctuating pH due to the disruption of electrostatic interactions. In contrast, the

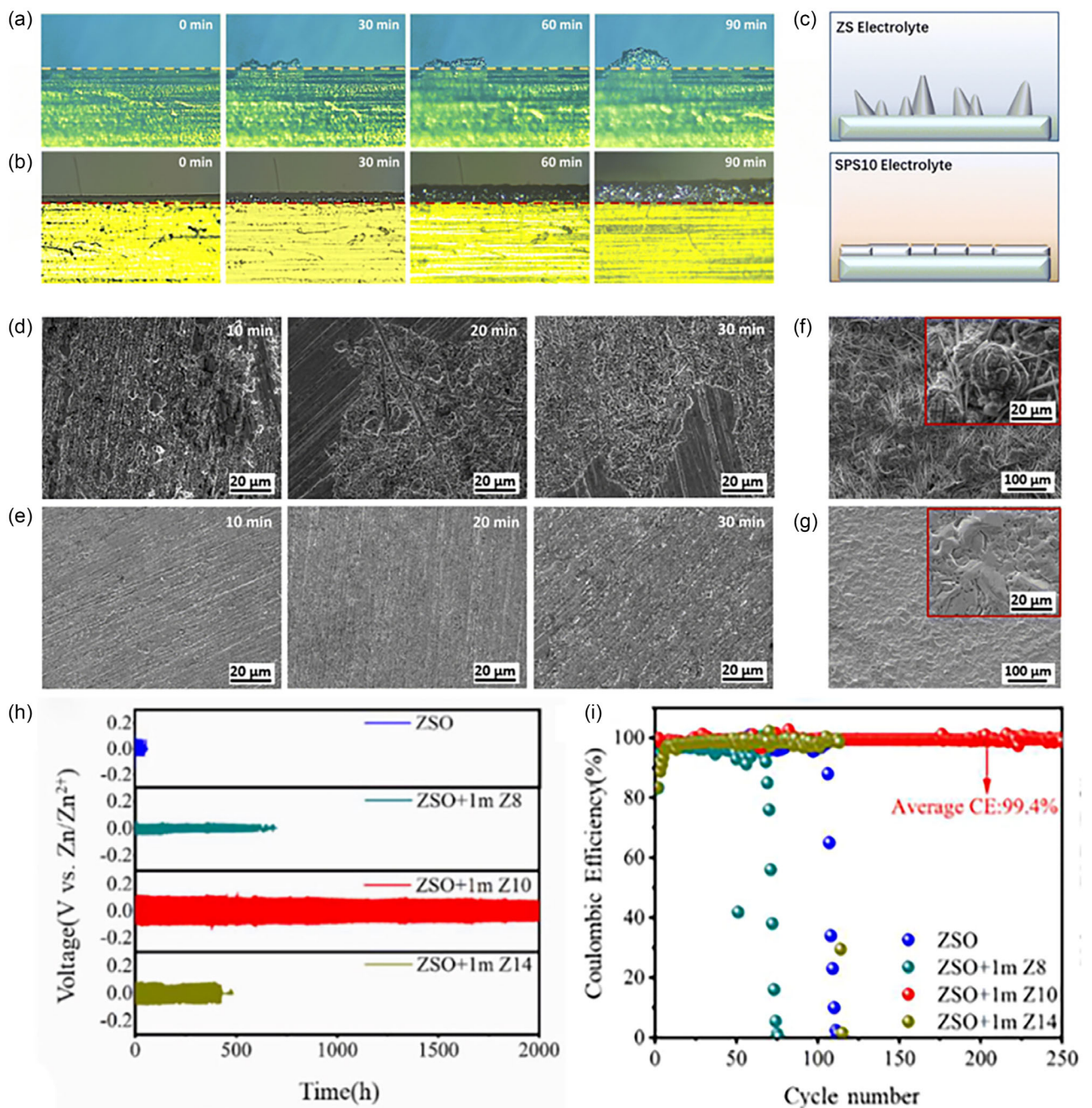


Figure 5. Characterization of electrodeposition morphology of Zn metal anode. In situ optical microscope images of Zn electrodeposition process at a current density of 5 mA cm^{-2} in a) ZS and b) SPS10 electrolytes. c) Schemes of Zn deposition in different electrolytes. SEM images of deposited Zn after different deposition time in d) ZS and e) SPS10 electrolytes. SEM images of cycled Zn anode after 50 cycles at a current density of 1 mA cm^{-2} and a capacity of 1 mA h cm^{-2} in symmetric cells (inset shows magnified SEM image) assembled using f) ZS and g) SPS10 electrolytes. Reproduced with permission.^[55] Copyright (2023), Energy & Environmental Science. h) Galvanostatic Zn plating/stripping of long-term cyclic stability of Zn||Zn symmetrical batteries with different electrolytes at a current density of 1 mA cm^{-2} and the area capacity of 1 mAh cm^{-2} . i) CE measurements of Zn||Cu batteries using the different electrolytes; The ZSO electrolyte with different concentrations of Z10 ($0.5, 1, 5, 10$ and 20 mmol L^{-1} , termed $0.5, 1, 5, 10$ and 20 m Z10 , respectively).^[56] Reprinted from Energy Storage Materials, Vol. 63, Li Tao, Kailin Guan, Rong Yang, Zhongxian Guo, Longyang Wang, Lei Xu, Houzhao Wan, Jun Zhang, Hanbin Wang, Linfeng Hu, Paul J. Dyson, Mohammad Khaja Nazeeruddin, Hao Wang, "Dual-protected zinc anodes for long-life aqueous zinc ion battery with bifunctional interface constructed by zwitterionic surfactants," Article No. 102981, Copyright (2023), with permission from Elsevier. CE, coulombic efficiency.

nonionizable nature of nonionic surfactants effectively avoids charge shielding effects and ion competition, enabling them to retain structural integrity and surface activity even in complex electrochemical environments. Polyethylene glycol (PEG)-based

compounds are representative examples of nonionic surfactants and are widely used due to their amphiphilic nature and strong interfacial activity. For instance, Zhang et al.^[60] introduced polyethylene glycol tert-octylphenyl ether (PEGTE) as an electrolyte

additive to construct an *in situ* passivation layer composed of honeycomb-structured ZnO on the zinc anode surface. This passivation layer not only facilitates uniform electric field distribution and guides homogeneous Zn^{2+} deposition but also effectively suppresses dendrite formation, thereby improving cycling

stability. As a result, $Zn \parallel Zn$ symmetric cells incorporating PEGTE exhibited excellent long-term performance under high areal capacity conditions, maintaining stable cycling for over 2400 h at 5 mAh cm^{-2} and exceeding 1300 h at 10 mAh cm^{-2} (Figure 6a,b).

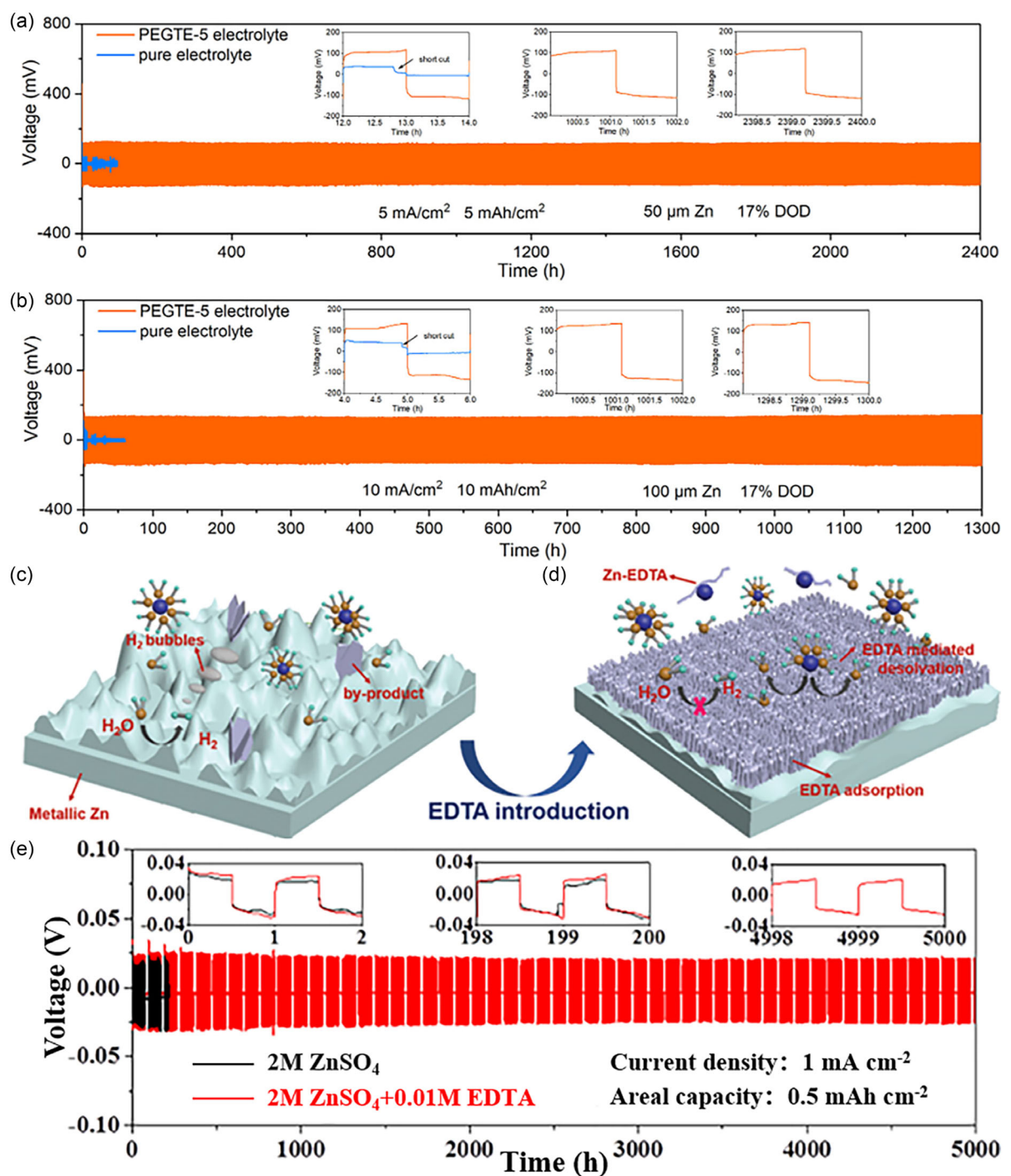


Figure 6. a,b) Cycling performance of the symmetric $Zn \parallel Zn$ cells at (a) 5 mA cm^{-2} and 5 mAh cm^{-2} and (b) at 10 mA cm^{-2} and 10 mAh cm^{-2} . Reproduced with permission.^[60] Copyright 2022, American Chemical Society. Schematic of Zn/electrolyte interphase behaviors during Zn plating in: c) $ZnSO_4$ electrolyte and d) EDTA-functionalized $ZnSO_4$ electrolyte. Reproduced with permission.^[64] Copyright (2021), Wiley-VCH. e) Dynamic measurement combining plating/stripping cycling at 1 mA cm^{-2} and 0.5 mAh cm^{-2} for 72 h and resting for 24 h for $Zn \parallel Zn$ symmetric cells with 2 M ZnSO_4 electrolyte or $2 \text{ M ZnSO}_4 + 0.01 \text{ M EDTA}$ electrolyte. Reproduced with permission.^[42] Copyright (2022), Wiley-VCH.

In contrast, water-soluble polymers such as polyvinyl alcohol (PVA) enhance electrolyte performance primarily by constructing 3D ion-conducting networks. Unlike approaches that rely on interfacial tension regulation, PVA utilizes its abundant hydroxyl groups to form dense hydrogen bonding and physical entanglements with water molecules and Zn^{2+} ions, thereby significantly improving ionic conductivity and effectively suppressing zinc dendrite formation. Studies have shown that the $-OH$ groups in PVA exhibit strong interactions with Zn^{2+} via hydrogen bonding, which contributes to stabilizing the electrode–electrolyte interface. In comparative experiments, Zn anodes soaked in electrolytes without PVA for 13 days exhibited pronounced surface roughness and corrosion, whereas those treated with PVA-containing electrolytes maintained a smoother and more uniform surface, indicating PVA's effectiveness in mitigating corrosion and suppressing HER.^[61]

Moreover, the 3D network formed by PVA not only enhances ion transport but also imparts excellent self-healing and antifreezing properties, allowing stable ion conduction across a wide temperature range.^[62,63] Notably, PVA also exhibits excellent adaptability to fluctuations in ionic strength and pH, primarily due to its neutral polymer backbone and highly polar functional groups, which contribute to its chemical stability. With low environmental sensitivity and superior structural tuning capabilities, PVA serves as an ideal functional additive for AZIBs, particularly under complex or fluctuating operating conditions, supporting their long-term stable operation.

2.1.2. Chelating Agent Additives

Chelating agents can coordinate with Zn^{2+} to form stable complexes, thereby regulating its solubility and migration behavior in the electrolyte. This coordination effectively suppresses side reactions and optimizes the deposition kinetics of zinc. Common classes of chelating agents include organic carboxylic acids, amino acids, aldehydes/ketones, and multidentate ligands. Zhang et al.^[64] demonstrated that the incorporation of tetrasodium ethylenediaminetetraacetate (Na_4EDTA) into $ZnSO_4$ -based electrolytes simultaneously suppresses both zinc dendrite formation and hydrogen evolution side reactions. Mechanistic investigations revealed that $EDTA^{4-}$ anions can adsorb onto the zinc electrode surface (Figure 6c,d), occupying active sites for the HER and thereby significantly inhibiting water decomposition. Additionally, $EDTA^{4-}$ facilitates the desolvation of $Zn(H_2O)_6^{2+}$ by stripping coordinated water molecules, promoting uniform Zn deposition. As a result, the battery achieved a high Coulombic efficiency of 99.5% at 5 mA cm^{-2} and exhibited a cycling life of over 2500 cycles at 2 mA cm^{-2} . Ou et al.^[42] introduced EDTA into $ZnSO_4$ aqueous electrolyte, where it displaced adsorbed water molecules on the zinc surface to form a stable chelating adsorption interface. This EDTA-derived chemisorbed layer significantly reduced direct contact between water and metallic Zn, lowering the corrosion rate by more than 50%. Moreover, its oxygen- and nitrogen-rich functional groups helped regulate zinc deposition kinetics, substantially improving

deposition uniformity. Under demanding cycling conditions of 1 mA cm^{-2} and 0.5 mAh cm^{-2} , the interfacial layer maintained excellent stability after 72 h of dynamic cycling and 24 h of rest, enabling highly reversible Zn plating/stripping behavior over 5000 h (Figure 6e). In addition, nitrogen-containing organic ligands such as urea and triethanolamine have shown strong chelating ability, improving Zn^{2+} stability in electrolyte and mitigating cathode dissolution. These multifunctional additives offer promising prospects for enhancing both anode and cathode performance in aqueous zinc battery systems.

2.1.3. Corrosion Inhibitor Additives

Corrosion inhibitors primarily function by forming a protective adsorption layer on the zinc surface, effectively suppressing side reactions with water, such as hydrogen evolution. These additives typically contain functional groups such as carboxyl, amino, or amide groups, which enable weak coordination or physical adsorption with Zn^{2+} , thereby extending battery lifespan. Common corrosion inhibitors include benzotriazole (BTA), imidazole derivatives, and similar compounds. Li et al.^[65] reported an organic molecule with both high zinc affinity and hydrophobicity—2-amino-6-trifluoromethoxybenzothiazole (TBA)—as a functional additive in $ZnSO_4$ -based electrolytes. In this molecule, the benzothiazole moiety strongly adsorbs onto the zinc anode surface, while the trifluoromethoxy group effectively blocks active water molecules. TBA preferentially adsorbs onto the zinc surface, generating a uniform electric field that regulates Zn^{2+} deposition, suppresses tip-induced field enhancement, and effectively inhibits dendrite growth. Additionally, it significantly lowers the nucleation overpotential, facilitating rapid Zn plating/stripping kinetics. The TBA-derived protective layer provided up to 99.1% corrosion inhibition for the zinc anode (Figure 7a–f). As a result, $Zn \parallel Zn$ symmetric cells exhibited stable cycling for over 1600 h at a current density of 5 mA cm^{-2} . Furthermore, $Zn \parallel Cu$ half cells maintained a high Coulombic efficiency of 99.25% after 300 cycles at 1 mA cm^{-2} . Wu et al.^[66] introduced 2-methylimidazole (Hmim) as an electrolyte additive, which enabled the *in situ* formation of a robust solid–electrolyte interphase (SEI) consisting of inorganic–organic Zn-rich compounds ($Zn_4SO_4(OH)_6/Zn(Hmim)$) (Figure 7g). Hmim exhibits strong zinc affinity, forming chelating complexes with Zn^{2+} that provide additional nucleation sites and promote uniform zinc deposition. Its coordination effect also alters the local ion diffusion environment, increases nucleation overpotential, and refines the initial Zn grain size. Moreover, the resulting composite interphase exhibits excellent chemical and thermal stability, effectively suppressing side reactions and dendrite growth. Consequently, the Hmim-modified electrolyte achieved a high Coulombic efficiency of 97.32% and stable cycling performance for up to 2000 h.

2.1.4. Multifunctional Organic Additives

In recent years, increasing attention has been given to organic molecules that simultaneously exhibit corrosion inhibition,

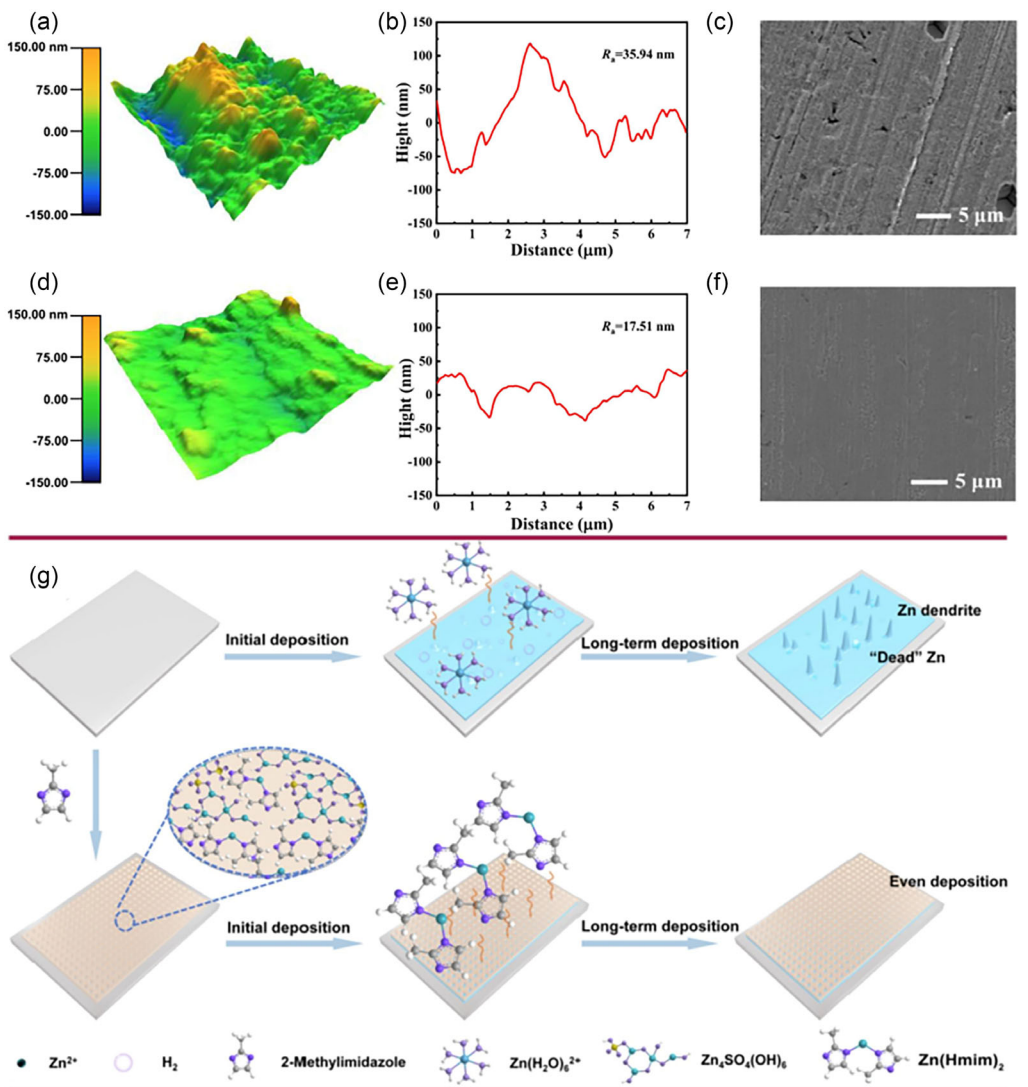


Figure 7. AFM and SEM images of Zn surface under different conditions: a–c) without TBA; d–f) with TBA.^[65] Reprinted from Corrosion Science, Vol. 246, Haohan Li, Yue Gan, Xiaohong Chen, Juan Wang, Taoqiang Ling, Bo Shang, Wenpo Li, Qian Li, "New strategy for zinc anode corrosion protection: Development of a benzothiazole-based inhibitor and its optimization for battery performance", Article No. 112762, Copyright (2025), with permission from Elsevier. g) Schematic illustrations of the effect of Hmim addition on Zn deposition.^[66] Reprinted from Chemical Engineering Journal, Vol. 452, Cuiping Wu, Chuang Sun, Kaixin Ren, Fenglei Yang, Yixun Du, Xingxing Gu, Qinghong Wang, Chao Lai, "2-methyl imidazole electrolyte additive enabling ultra-stable Zn anode," Article No. 139465, Copyright (2022), with permission from Elsevier. AFM, atomic force microscopy.

complexation, and interfacial regulation capabilities. For example, amino acid molecules containing multiple carboxyl and amino groups can form stable complexes with Zn^{2+} while adsorbing onto the anode surface to suppress side reactions. Moreover, their excellent water solubility and biodegradability make them attractive candidates for green electrolyte design. Meng et al.^[67] employed cysteine (Cys) as a multifunctional electrolyte additive to stabilize the zinc anode. Experimental and theoretical analyses demonstrated that Cys, containing various polar functional groups, strongly interacts with both Zn^{2+} ions and metallic zinc. These interactions facilitate the reconstruction of the solvation structure and optimization of the anode–electrolyte interphase (AEI). Such synergistic modulation improves the deposition kinetics of Zn^{2+} , effectively inhibits dendrite formation and parasitic

reactions, and significantly enhances the long-term stability of the zinc anode. As a result, $\text{Zn} \parallel \text{Zn}$ symmetric cells achieved an ultralong cycle life exceeding 2300 h under standard conditions, with cycling performance improved by more than tenfold under various operating conditions. Even under harsh conditions of high current density (5 mA cm^{-2}) and high areal capacity (5 mAh cm^{-2}), the zinc anode maintained a cumulative plating capacity of up to 1.36 Ah and a high Coulombic efficiency of 99.4%. Zhang et al.^[68] proposed an electrochemical double layer (EDL) optimization strategy based on molecular adsorption to regulate the interfacial microenvironment by introducing ellagic acid (EA) into the electrolyte. The EA molecules exhibit strong interactions with the zinc surface and preferentially adsorb onto the Zn (002) crystal plane, thereby forming an *in situ* physical

interface layer with shielding capabilities. This adsorbed layer performs multiple functions: it acts as a barrier to $\text{H}_2\text{O}/\text{H}^+$, effectively suppressing parasitic reactions, while also facilitating uniform Zn^{2+} ion migration, leading to the dense and oriented deposition of the Zn (002) plane. As a result, the reversibility of zinc plating/stripping and interfacial stability are significantly enhanced. Electrochemical performance evaluations demonstrate that $\text{Zn}||\text{Zn}$ symmetric cells maintain stable cycling for over 300 h under variable current densities ranging from 1 to 20 mA cm^{-2} . $\text{Zn}||\text{Cu}$ half cells exhibit a high Coulombic efficiency of 99.53% after 1000 cycles at 5 mA cm^{-2} and 1 mAh cm^{-2} . Furthermore, $\text{Zn}||\text{MnO}_2$ full cells retain 72.9% of their capacity after 2000 cycles at a current density of 2 A g^{-1} . Zhong et al.^[69] introduced monosodium glutamate (MSG) as an electrolyte additive, which effectively suppressed dendrite growth and hydrogen evolution by reconstructing the Zn anode/electrolyte interface. Glutamate anions preferentially adsorbed onto corrosion- and hydrogen-evolution-active sites on the zinc surface, significantly reducing the likelihood of side reactions. This adsorption also facilitated redistribution of the Zn^{2+} flux and promoted the desolvation of $[\text{Zn}(\text{H}_2\text{O})_6]^{2+}$, enabling uniform zinc deposition at low overpotentials. Owing to the optimized interfacial structure, $\text{Zn}||\text{Zn}$ symmetric cells demonstrated stable cycling for over 1700 h at 5 mA cm^{-2} and 5 mAh cm^{-2} , with voltage hysteresis below 60 mV. Even under demanding conditions of high current density (9.11 mA cm^{-2}) and limited zinc supply (80% utilization), the cell remained stable for 460 h. In addition, Liang et al.^[70] introduced a multifunctional organic additive, pyrocatechol violet (PV), into baseline ZnSO_4 electrolyte to *in situ* construct a stable protective layer on the zinc anode surface. This protective layer effectively buffers the pH fluctuations at the anode/electrolyte interface, thereby significantly suppressing the HER. Moreover, the modified zinc anode exhibits a preferred orientation along the (101) crystal plane, resulting in a denser and more uniform deposition morphology with enhanced interfacial stability. Electrochemical tests demonstrate that the $\text{Zn}||\text{Zn}$ symmetric cell achieves an ultralong cycling life of up to 4000 h at 1 mA cm^{-2} and 1 mA h cm^{-2} and maintains stable operation for 1300 h even at 5 mA cm^{-2} . The $\text{Zn}||\text{Cu}$ half cell retains a Coulombic efficiency close to 100% after 1500 h of cycling, indicating excellent Zn stripping/plating reversibility. Furthermore, the $\text{Zn}||\text{MnO}_2$ full cell delivers superior electrochemical performance compared to the control without additive, confirming the effectiveness of this strategy in enhancing the practical applicability of AZIBs. Additionally, Hao et al.^[71] reported a “set-it-and-forget-it” electrolyte design strategy using a trifunctional additive, $\text{C}_3\text{H}_7\text{Na}_2\text{O}_6\text{P}$, capable of continuous activity during battery resting phases. This additive modulates hydrogen ion concentration and reduces free water activity, thereby suppressing hydrogen evolution. Moreover, it induces the *in situ* formation of a self-healing SEI before battery operation, simultaneously inhibiting oxygen-induced corrosion and zinc dendrite growth. Benefiting from this strategy, the battery achieved a Zn plating/stripping efficiency of 99.6% at a high depth of discharge (85%), and the pouch full cell constructed with lean electrolyte maintained

95.5% of its capacity after 500 cycles—setting a new benchmark for cycle life.

2.2. Inorganic Additives

Inorganic additives play a vital role in AZIBs due to their structural simplicity, wide availability, excellent thermal stability, and ability to regulate the ionic environment of the electrolyte.^[36,72] Typically introduced in the form of metal salts, inorganic acids/bases, or oxides, these additives serve to modulate the pH value, optimize the solvation structure of Zn^{2+} , enhance ionic conductivity, and improve the stability of the electrode/electrolyte interface.^[37,73–76] Based on their primary functions, inorganic additives can be broadly categorized into the following types.

2.2.1. Metal Salt Additives

Metal salt additives exhibit significant effects in regulating the solvation structure and electrochemical deposition behavior of Zn^{2+} , thereby effectively suppressing parasitic reactions such as hydrogen evolution and the growth of zinc dendrites. Commonly used metal salts include $\text{Al}_2(\text{SO}_4)_3$,^[77,78] MgSO_4 ,^[79] MnSO_4 ,^[80,81] and CoSO_4 .^[82] The metal cations in these salts compete with Zn^{2+} for coordination with water molecules, thus weakening Zn^{2+} hydration and reducing the activity of water decomposition reactions.^[83] For instance, additives containing Ni^{2+} , Cu^{2+} , or Pd^{2+} are mainly employed to modulate zinc dissolution or deposition behavior and effectively inhibit dendrite formation. Cations such as Na^+ , Mg^{2+} , and Al^{3+} can synergistically intercalate or induce interfacial reactions, improving the capacity, voltage plateau, and interfacial stability of ZIBs, thereby enhancing overall electrochemical performance.^[79,84,85] Mn^{2+} ions not only regulate the deposition morphology of Zn but also compensate for the dissolution of Mn^{2+} from the cathode during cycling, leading to improved cycle stability.^[86] Guo et al.^[87] demonstrated that lithium chloride (LiCl) additive can effectively suppress dendrite growth and stabilize the zinc metal anode. Specifically, Li^+ cations preferentially form a $\text{Li}_2\text{O}/\text{Li}_2\text{CO}_3$ layer on the zinc surface, creating a shielding effect that inhibits dendrite formation. Meanwhile, Cl^- anions reduce electrode polarization and facilitate ion transport. The inclusion of LiCl in the electrolyte significantly enhanced long-term cycling performance in asymmetric cells. In addition, rare-earth elements such as Ce^{3+} exhibit strong charge shielding capabilities, enabling the formation of an electrostatic shielding layer at the anode surface to homogenize the local electric field and suppress dendrite growth. Hu et al.^[88] introduced CeCl_3 as an additive in ZIBs and constructed a dynamic electrostatic shielding layer around zinc protrusions (**Figure 8a**), which effectively guided uniform zinc deposition. Benefiting from this strategy, $\text{Zn}||\text{Zn}$ symmetric cells achieved a prolonged cycle life of 2600 h at a current density of 2 mA cm^{-2} , and an accumulated areal capacity as high as 3.6 Ah cm^{-2} at 40 mA cm^{-2} , with a Coulombic efficiency of \approx 99.7%. Notably, the full $\text{Zn}||\text{LiFePO}_4$ cell incorporating CeCl_3 exhibited significantly improved capacity retention compared to its additive-free counterpart.

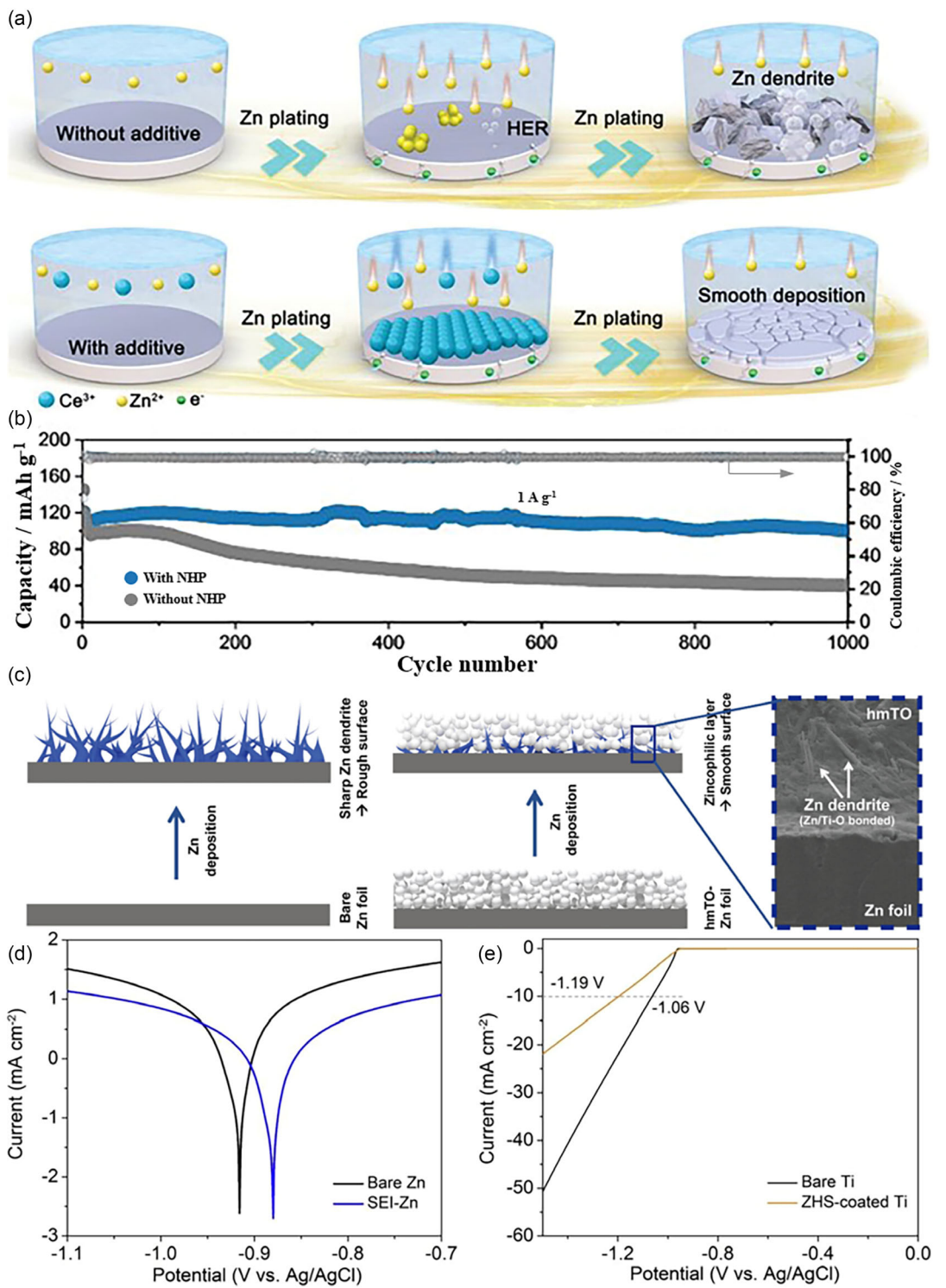


Figure 8. a) Schematic illustration of the Zn deposition process modulated by the CeCl₃ additive, highlighting its role in guiding uniform nucleation. Reproduced with permission.^[88] Copyright (2022), Wiley-VCH. b) Electrochemical performance of Zn||MnO₂ full cells at 1 A g⁻¹ under high mass loading conditions, demonstrating enhanced stability with electrolyte additives. Reproduced with permission.^[95] Copyright (2022), Wiley-VCH. c) Schematic of Zn dendrite growth on the bare anode and its suppression through hierarchical mesoporous TiO₂ (hmTO) layer coating, enabling uniform deposition.^[102] Reprinted from Applied Surface Science, Vol. 606, Nibagani Naresh, Suyoon Eom, Su Hwan Jeong, Sang Jun Lee, So Hyeon Park, Jonghee Park, Jou-Hyeon Ahn, Joo-Hyung Kim, Young Hwa Jung, "Dendrite-free Zn anodes enabled by a hierarchical zincophilic TiO₂ layer for rechargeable aqueous zinc-ion batteries," Article No. 154932, Copyright (2022), with permission from Elsevier. d) Tafel plots comparing the corrosion behavior of SEI-modified Zn and bare Zn electrodes, recorded at a scan rate of 1.0 mV s⁻¹. e) Linear sweep voltammetry curves of bare Ti and ZHS-coated Ti electrodes, illustrating reduced hydrogen evolution on the protected surface at 1.0 mV s⁻¹.^[110] Reprinted from Chemical Engineering Journal, Vol. 431, Part 1, Wentao Yuan, Guoqiang Ma, Xueyu Nie, Yuanyuan Wang, Shengli Di, Liubin Wang, Jing Wang, Shigang Shen, Ning Zhang, "In-situ construction of a hydroxide-based solid electrolyte interphase for robust zinc anodes," Article No. 134076, Copyright (2021), with permission from Elsevier.

2.2.2. pH-Regulating Additives

The pH of the electrolyte plays a crucial role in determining the electrochemical kinetics of Zn as well as its side reactions, such as hydrogen evolution and $\text{Zn}(\text{OH})_2$ precipitation.^[89,90] By introducing appropriate acidic or alkaline additives, the electrolyte pH can be precisely tuned to optimize the solvation structure of Zn^{2+} and interfacial reaction behavior. For instance, the addition of H_2SO_4 can lower the electrolyte pH, thereby suppressing the formation of $\text{Zn}(\text{OH})_2$ precipitates and maintaining the activity of the electrode surface. However, the acid concentration must be carefully controlled to avoid accelerating the HER.^[91] In contrast, alkaline additives promote the formation of hydroxy complexes such as $[\text{Zn}(\text{OH})_4]^{2-}$, which help mitigate hydrogen evolution during the reduction process and stabilize the interfacial structure.^[92,93] Moreover, phosphate buffer solutions can maintain a relatively stable electrolyte pH during cycling, effectively enhancing the interfacial stability of the Zn anode and improving the long-term cycling performance of the battery.^[94] Zhang et al.^[95] introduced an inexpensive and efficient additive, ammonium dihydrogen phosphate (NHP), into dilute aqueous ZnSO_4 electrolytes to buffer the pH and suppress dendrite growth and side reactions during cycling. Both experimental and theoretical results demonstrated that the Zn-philic NH_4^+ ions are preferentially adsorbed on the Zn surface to form a “shielding effect,” which blocks direct contact between water molecules and the Zn surface. This leads to dendrite-free Zn deposition and suppression of hydrogen-related side reactions. Notably, the pH-buffering species NH_4^+ and H_2PO_4^- maintain the concentration balance of H^+ and OH^- at the electrolyte-electrode interface, offering a secondary layer of protection for the Zn electrode. As a result, the NHP additive enables highly reversible Zn plating/stripping: $\text{Zn}||\text{Zn}$ symmetric cells using NHP exhibit stable cycling for 2100 h at 1 mA cm^{-2} , 1900 h at 4 mA cm^{-2} , and 930 h at 10 mA cm^{-2} . Furthermore, $\text{Zn}||\text{Cu}$ asymmetric cells show a high average Coulombic efficiency of 99.4% over 1000 cycles (Figure 8b).

2.2.3. Inorganic Oxide Nanoparticle Additives

Inorganic oxide nanoparticles have attracted significant attention in recent years as electrolyte additives for regulating the Zn anode interface.^[96,97] These additives can either physically adsorb onto the Zn surface or participate in interfacial reactions, thereby modulating Zn^{2+} ion migration, nucleation processes, and deposition morphology. Such regulation enhances interfacial stability and extends the cycling life of zinc-based batteries.^[98,99] Among them, TiO_2 nanoparticles, which possess abundant surface active sites, can adsorb Zn^{2+} ions and act as heterogeneous nucleation centers. This facilitates uniform and nonlocalized Zn deposition, effectively suppressing dendrite growth.^[100,101] Naresh et al.^[102] developed a hierarchical nanostructured layer composed of mesoporous Zn-affinitive TiO_2 nanoparticles (Figure 8c). This layered TiO_2 coating on the Zn surface (hmTO-Zn) plays a critical role in mitigating dendrite formation and significantly enhances

the electrochemical performance of ZIBs. In rechargeable AZIBs with a configuration of hmTO-Zn| $\text{Zn}(\text{CF}_3\text{SO}_3)_2|\text{V}_2\text{O}_5$, the battery demonstrated ultralong cycling life and excellent rate capability. Compared with the bare Zn anode (44 mAh g^{-1} after 5000 cycles), the battery with the hmTO-Zn electrode maintained a high capacity of 102 mAh g^{-1} after 5000 cycles at a high current density of 5000 mA g^{-1} , with nearly 100% Coulombic efficiency. In addition, SiO_2 nanoparticles exhibit excellent Zn^{2+} adsorption capability and interfacial wettability regulation due to their high specific surface area and surface hydroxyl groups.^[103] These properties help achieve uniform Zn^{2+} distribution and stable deposition behavior. Guo et al.^[104] employed a hydrothermal method to construct an *in situ* $\text{ZnO}-\text{SiO}_2$ composite interfacial phase ($\text{Zn}@\text{ZSCP}$), forming a dual-function protective layer. In this structure, the hydrophilic SiO_2 layer lowers the nucleation energy barrier, while the ZnO layer contributes to electric field redistribution and induces uniform Zn nucleation. The $\text{Zn}@\text{ZSCP}$ -modified symmetric cell exhibited a cycling lifespan of up to 2500 h. Even under a high current density of 8 mA cm^{-2} , the symmetric cell maintained a stable cycling life exceeding 2000 h.

2.2.4. Halide and Other Anionic Additives

In addition to cation-regulating strategies, inorganic anionic additives have also demonstrated significant advantages in enhancing the interfacial stability of Zn anodes. These anions typically regulate Zn deposition behavior, reduce the rate of side reactions, and extend battery cycling life by forming stable complexes with Zn^{2+} or inducing the *in situ* formation of protective surface layers.^[95,105] Li et al.^[106] discovered that trace amounts of fluoride ions (F^-) introduced into the electrolyte could induce the *in situ* formation of a dense ZnF_2 passivation layer on the Zn anode surface. This layer effectively isolates water molecules and suppresses hydrogen evolution, significantly improving the cycling stability and Coulombic efficiency of Zn-based batteries. Furthermore, Chen et al.^[107] developed a uniform and thin SEI film rich in ZnF_2 and ZnS . This SEI layer not only suppresses interfacial side reactions and dendritic Zn growth but also optimizes Zn^{2+} diffusion at the interface, enabling stable Zn^{2+} transport and deposition along the Zn (002) crystal plane. As a result, $\text{Zn}|\text{Zn}$ symmetric cells maintained stable plating/stripping for up to 5000 h, while $\text{Zn}|\text{Cu}$ half cells exhibited excellent cycling stability at a current density of 5.0 mA cm^{-2} over 1500 cycles, with a high Coulombic efficiency of $\approx 99.8\%$. Phosphate ions (PO_4^{3-}) can also form electrochemically stable composite interfacial structures with Zn^{2+} , regulate Zn deposition behavior, and effectively suppress dendrite formation.^[36,108] Additionally, nitrate ions (NO_3^-) can indirectly influence the Zn deposition process by modulating the pH and ionic strength of the electrolyte, thereby enhancing cycling stability.^[28,109] Notably, Yuan et al.^[110] introduced sulfate additives (e.g., ZnSO_4 or Na_2SO_4) into a mildly concentrated aqueous electrolyte ($2 \text{ M } \text{Zn}(\text{OTf})_2$), leading to the *in situ* formation of a stable, Zn^{2+} -conductive SEI layer composed of zinc hydroxide sulfate hydrate. During initial cycling, a self-limiting chemical reaction between SO_4^{2-} , Zn^{2+} , and OH^- (generated from the

HER) induces the formation of a compact interphase. This SEI effectively prevents direct contact between Zn and the bulk electrolyte, thereby inhibiting continuous hydrogen evolution and Zn corrosion (Figure 8d,e), while simultaneously ensuring uniform Zn^{2+} migration. Consequently, $Zn||Cu$ cells demonstrated high reversibility with over 600 cycles and a Coulombic efficiency of 99.8% at 1.0 mA cm^{-2} . $Zn||Zn$ symmetric cells exhibited unprecedented cycling stability with a lifespan exceeding 2000 h. Moreover, the presence of this SEI layer significantly enhanced the long-term operation of full $Zn||V_2O_5\cdot nH_2O$ batteries. In summary, inorganic anionic additives play a critical role in stabilizing the Zn anode interface and suppressing parasitic reactions through multiple mechanisms, including modulation of Zn^{2+} coordination structures, induction of protective interfacial layers, and regulation of interfacial charge distribution. These strategies represent a promising and indispensable direction for the development of high-performance AZIBs.

2.3. Ionic Liquid Additives

ILs, as a novel class of organic additives, have garnered increasing attention in AZIBs in recent years. Due to their excellent ionic conductivity, low volatility, and high thermal stability, they exhibit unique advantages under high-temperature and extreme operating conditions. For instance, Yu et al.^[111] reported the incorporation of 1-ethyl-3-methylimidazolium bis(fluorosulfonyl)imide ([EMIM][FSI]) as a “water-in-salt”-type IL diluent into the electrolyte, which effectively reduced water activity and suppressed side reactions. During the zinc deposition process, the [EMIM]⁺ cation and FSI⁻ anion alleviated the tip effect and regulated the formation of the SEI, thereby promoting uniform zinc deposition. Benefiting from the chemical and electrochemical stability of IL, the IL-doped aqueous electrolyte (IL-AE) enabled the $Zn||Zn_{0.25}V_2O_5\cdot nH_2O$ battery to operate stably even at a challenging temperature of 60 °C, retaining over 85% of its capacity after 400 cycles. Additionally, Chen et al.^[112] employed 1-butyl-3-methylimidazolium trifluoromethanesulfonate ([BMIM]OTF), a water-soluble IL with an ultralow melting point, as an electrolyte additive, achieving significant performance enhancements. Results showed that the addition of [BMIM]OTF to a 3 M $Zn(OTF)_2$ aqueous electrolyte had minimal effect on ionic conductivity at room temperature, while markedly improving the electrolyte’s low-temperature adaptability. Moreover, [BMIM]OTF preferentially adsorbs onto the zinc anode surface, modulates the Zn^{2+} solvation structure, reduces zinc corrosion activity, and induces the formation of an organic/inorganic hybrid SEI. This SEI exhibits both zincophilicity and hydrophobicity, facilitating a reduced nucleation overpotential for zinc deposition, improved interfacial charge transfer kinetics, uniform deposition, and effective suppression of side reactions. The $Zn||Zn$ symmetric cell using the [BMIM]OTF-modified electrolyte demonstrated excellent cycling stability even at an ultrahigh areal capacity of 25 mAh cm^{-2} . Furthermore, full cells assembled with an aluminum vanadate cathode maintained outstanding electrochemical performance under extreme low-temperature conditions down

to -30°C . Zhong et al.^[113] proposed a novel room-temperature liquid zinc salt, zinc-coordinated IL ($(EMIM)_5Zn(OTF)_7$), for constructing AZIBs operable under all-climate conditions. When dissolved in an ethylene glycol (EG)/water mixed solvent (volume ratio 6:4) at a concentration of 0.261 mol kg^{-1} , the resulting electrolyte exhibited a freezing point below -100°C , indicating excellent low-temperature tolerance. The synergistic interaction between $(EMIM)_5Zn(OTF)_7$ and EG molecules reconstructs the Zn^{2+} solvation structure, reduces the coordination number of water molecules in the primary solvation shell, and effectively suppresses side reactions such as hydrogen evolution. As a performance validation, both $Zn||Zn$ symmetric cells and $Zn||PANI$ full cells using this electrolyte demonstrated outstanding cycling stability, operating reliably over a wide temperature range from -40 to 60°C . Even under high zinc utilization (40%), the battery retained 80% of its capacity and maintained stable cycling for over 70 cycles.

2.4. Composite Additives

With continuous progress in the research of AZIBs, the limitations of single-type electrolyte additives in enhancing ionic conductivity, stabilizing electrode interfaces, and suppressing zinc dendrite growth have gradually become apparent. To overcome these challenges, researchers have proposed the synergistic application of two or more functional additives to construct composite additive systems.^[96] Among them, organic–inorganic composites and IL–inorganic composites have emerged as two representative research directions.^[114,115] These composite additives, through multiple cooperative mechanisms, can significantly enhance the overall performance and cycling stability of AZIBs.^[51,116]

2.4.1. Organic–Inorganic Composite Additives

Organic–inorganic composite additives exhibit significant synergistic effects in AZIBs by combining the interfacial regulation capabilities of organic molecules with the structural stability of inorganic materials. These additives not only facilitate the formation of efficient Zn^{2+} transport pathways and enhance the ionic conductivity of the electrolyte but also optimize the Zn^{2+} deposition behavior on the anode surface, effectively suppressing dendrite formation. Moreover, the composite interfacial layer constructed through the cooperation of organic and inorganic components can enhance electrode–electrolyte interface stability, inhibit side reactions such as hydrogen evolution, and thereby promote reversible Zn plating/stripping processes, significantly improving the cycling efficiency and lifespan of the battery. For instance, Zafar et al.^[117] developed an organic–inorganic hybrid cathode (APA-NVO) by intercalating amino polyethylene glycol amine (APA) into ammonium vanadate (NVO) layers, thereby significantly enhancing the electrochemical performance. The incorporation of APA not only expanded the interlayer spacing, facilitating Zn^{2+} diffusion, but also enabled reversible coordination between the amino groups and Zn^{2+} ions,

effectively suppressing interfacial side reactions. X-ray photoelectron spectroscopy (XPS) and electrochemical impedance spectroscopy analyses confirmed a marked reduction in charge transfer resistance, indicating mitigated parasitic reactions. Operating at a high voltage of 1.9 V, the hybrid cathode demonstrated excellent cycling stability, retaining 94% of its capacity after 1200 cycles, underscoring the synergistic role of the organic–inorganic architecture in enhancing both electrochemical performance and interfacial stability. Similarly, Ma et al.^[118] developed an organic (ethylenediamine, EDA)–inorganic (vanadium oxide) hybrid cathode that demonstrates ultrahigh rate capability and long cycle life. The EDA molecules, intercalated between the vanadium oxide layers, increase the interlayer spacing, thus promoting efficient Zn²⁺-ion migration. EDA also functions as a bidentate ligand in the Zn²⁺ storage process, leading to enhanced specific capacity and remarkable cycling stability. This hybrid design not only improves the ionic conductivity but also alleviates side reactions typically encountered in pure vanadium oxide systems. The increased interlayer spacing minimizes issues related to phase transitions and vanadium dissolution, while EDA’s chelating ability helps suppress unwanted side reactions, contributing to a stable and reversible zinc-ion storage mechanism. Furthermore, Zhang et al.^[119] provided a comprehensive review of organic–inorganic composite cathode materials in AZIBs, highlighting their potential in significantly enhancing both energy density and cycle life. These studies collectively underscore the broad application prospects of organic–inorganic composite additives in improving the overall performance of AZIBs and suggest that further exploration of their regulation mechanisms and structural designs is highly warranted.

2.4.2. Ionic Liquid–Inorganic Composite Additives

Due to their high ionic conductivity, wide ESW, and excellent thermal stability, ILs have shown promising potential in AZIBs. However, the high cost of ILs and their tendency to induce unfavorable interfacial reactions with the zinc anode limit their feasibility as standalone additives. By forming composite additives with inorganic components, these limitations can be effectively overcome through complementary functionalities, enabling the synergistic enhancement of battery performance and interfacial stability. ILs can provide low-impedance migration pathways to facilitate Zn²⁺ diffusion,^[120,121] while inorganic particles help stabilize interfacial structures and mitigate corrosion reactions.^[97,102] The combined action of ILs and inorganic additives enables regulation of solvation structures and electric field distribution, thereby optimizing zinc deposition behavior and suppressing dendrite growth.^[122] For example, Shen et al.^[123] introduced a functional IL, 1-butyl-3-methylimidazolium hexafluorophosphate ([BMIM]PF₆), into AZIBs and proposed a synergistic mechanism combining interfacial regulation and solvation modulation. The [BMIM]⁺ cations preferentially adsorb onto the protrusions of the zinc anode surface, thereby weakening the local electric field and promoting uniform Zn²⁺ deposition, effectively suppressing dendrite growth. Meanwhile, PF₆⁻ anions participate in the Zn²⁺ solvation structure by partially replacing water molecules, which reduces the activity of free water, mitigates hydrogen evolution and side reactions, and enhances interfacial stability. In situ optical microscopy revealed that in the baseline electrolyte (BE) (Figure 9a), zinc dendrites began to emerge after 5 min of deposition, developed into irregular prismatic and dendritic structures after 10 min, and evolved into mossy dendrites after 15 min,

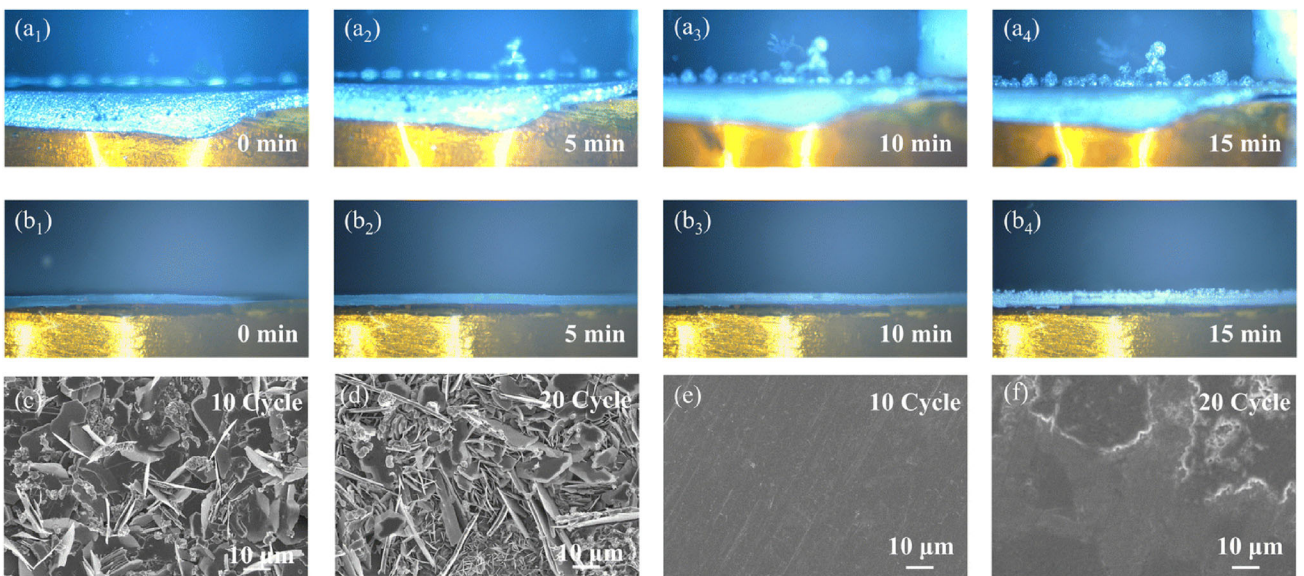


Figure 9. In situ optical microscopy images of Zn deposition in a) BE and b) [BMIM]PF₆/BE systems at various deposition durations at 10 mA cm⁻². SEM images of the Zn anode after c) 10 and d) 20 cycles in the BE system. SEM images of the Zn anode after e) 10 cycles and f) 20 cycles in the [BMIM]PF₆/BE system.^[123] Used with permission of Royal Society of Chemistry, from “A multifunctional IL additive providing a solvation structure and electrostatic shielding layer for highly stable aqueous zinc ion batteries,” Chen Shen, Yuxin Zhang, Xiang Li, Peng Guo, Xiang Zeng, Kangqi Ni, Rufeng Cao, Zhenguo Wang, Zhiliang Wang, and Lin Qin, Journal of Materials Chemistry A, Vol. 13, 2025, pp. 2174–2186; permission conveyed through Copyright Clearance Center, Inc.

indicating highly nonuniform deposition. In contrast, with the addition of [BMIM]PF₆ (Figure 9b), the zinc surface remained smooth and flat throughout the deposition process, with no observable dendrite formation. SEM analysis further confirmed this behavior: in the BE system (Figure 9c,d), the zinc surface exhibited rough, layered dendrites accompanied by accumulated byproducts, whereas in the [BMIM]PF₆-containing electrolyte (Figure 9e,f), the electrode surface was dense and uniform with no detectable byproducts. These results suggest that the additive facilitates the formation of a stable electrostatic shielding layer at the interface, effectively suppressing both dendritic growth and parasitic reactions. As a result, Zn||Zn symmetric cells exhibited a cycle life exceeding 1000 h at a current density of 4 mA cm⁻², and Zn||NH₄V₄O₁₀ full cells maintained 92.7% of their capacity after 3000 cycles at a high current density of 10 A g⁻¹. The IL-inorganic composite strategy offers a promising avenue for improving the overall performance of AZIBs. However, further investigations are needed to elucidate the underlying mechanisms and to guide the rational design of such systems.

Composite additives, by integrating the advantages of different additive types, provide a novel approach for electrolyte design in AZIBs. Recent studies have demonstrated that well-designed organic-inorganic or IL-inorganic composite systems have achieved breakthroughs in several aspects, such as enhanced cycling stability, dendrite suppression, and improved ionic conductivity.^[51] However, challenges remain for their practical application, including potential incompatibilities between components, increased complexity of interfacial reactions, uncertainty in long-term stability, as well as complicated synthesis processes and high production costs. Future research efforts should focus on in-depth mechanistic studies of composite interactions, optimization of interfacial regulation strategies, and comprehensive evaluation of scalability and economic feasibility, in order to accelerate the development of high-performance and cost-effective AZIBs.

In this section, we present a comprehensive overview of the classification of electrolyte additives for AZIBs, along with their underlying mechanisms for enhancing battery performance. These additives—including organic and inorganic compounds, ILs, and composite systems—play critical roles in significantly improving the cycling stability, Coulombic efficiency, and energy density of AZIBs through their distinct regulatory mechanisms. To facilitate a clearer understanding of the functional roles and performance advantages of different additive types, a summary table (Table 1) is provided below, outlining the major categories, representative examples, and key functions of various electrolyte additives.

3. Mechanisms of Electrolyte Additives in AZIBs

In recent years, as AZIBs have gained increasing attention for energy storage applications, several strategies have been proposed to address their key challenges—namely, poor electrolyte

stability, zinc dendrite growth, and limited cycle life. Among these, electrolyte additives have emerged as a particularly promising approach due to their low cost, operational flexibility, and significant performance-enhancing effects.^[18,19,124] This article systematically explores the fundamental mechanisms by which electrolyte additives function to improve the overall performance of AZIBs. Specifically, it discusses how these additives contribute to enhancing electrolyte stability, suppressing zinc dendrite formation, improving cycling performance, and increasing both energy density and efficiency of the batteries.

3.1. Enhancing Electrolyte Stability

Aqueous electrolytes have been widely employed in energy storage systems due to their high safety, low cost, and environmental friendliness. However, their ESW is inherently limited by the thermodynamic decomposition potential of water (\approx 1.23 V). In practical applications, this narrow ESW makes aqueous electrolytes prone to parasitic reactions such as hydrogen and oxygen evolution, which severely impact the energy efficiency, cycling stability, and safety of the batteries.^[125–128] To overcome these bottlenecks, various additive strategies have been proposed, ranging from molecular structure regulation to interfacial engineering, aiming to broaden the ESW and suppress side reactions in aqueous electrolytes. On the one hand, constructing hydrophobic interfaces has proven effective in expanding the ESW. The introduction of surfactants, for example, enables the formation of an orderly hydrophobic layer at the electrode/electrolyte interface, which repels water molecules from approaching the electrode surface and thereby suppresses the HER.^[129,130] Jing et al.^[131] used sodium dodecyl sulfate (SDS) as an electrolyte additive. Due to its intrinsic hydrophobicity, SDS formed a dynamic electrostatic shielding layer and a unique hydrophobic interface on the anode surface (Figure 10a). This effectively inhibited surface corrosion, hydrogen evolution, and dendrite growth, without sacrificing Zn²⁺ deposition kinetics. As a result, Zn||Zn symmetric cells incorporating SDS exhibited an extended cycling life of up to 2000 h (1 mA cm⁻², 1 mAh cm⁻²) (Figure 10b). In another study, SPS, an anionic surfactant, was employed as an additive. Unlike other conventional surfactants, SPS had a negligible impact on the bulk electrolyte structure. Its introduction significantly reduced zinc surface corrosion, hydrogen evolution, and dendrite growth. Notably, in a Zn||Zn pouch cell with an area of 3 × 5 cm² (replacing traditional coin-type cells), a cumulative capacity exceeding 12,000 mAh was achieved, demonstrating excellent electrochemical stability and scalability.^[55] On the other hand, regulating the hydrogen bond network among water molecules is also an effective way to enhance the ESW. The addition of highly polar organic solvents such as dimethyl sulfoxide (DMSO) and glycerol can disrupt hydrogen bonding between water molecules, reducing water's electrochemical activity and thereby suppressing gas-evolving side reactions.^[132,133] Cao et al.^[132] introduced DMSO into a ZnCl₂-H₂O dilute electrolyte system, which effectively suppressed both water decomposition and zinc dendrite formation. Due to its high Gutmann donor

Table 1. Electrolyte additives for AZIBs: Classification and functions.

Type	Additives	Effects	References
Organic	TMA ₂ SO ₄	Inhibit zinc dendrite growth	[53]
	SPS	Oriented Zn deposition and enhanced surface smoothness	[55]
	PEGTE	Electric field homogenization	[60]
	Na ₄ EDTA	Suppress zinc dendrite formation	[64]
	TBA	Enhanced Zn plating/stripping kinetics	[65]
	Hmim	Increase the zinc nucleation overpotential	[66]
	Cys	Adjust the solvation structure	[67]
	EA	Molecular adsorption for interface regulation	[68]
	PV	In situ formed stable protective layer	[70]
	C ₃ H ₇ Na ₂ O ₆ P	In situ formation of a self-healing SEI	[71]
Inorganic	Al ₂ (SO ₄) ₃	Expand the electrolyte voltage window	[77]
	MnSO ₄	Suppress capacity fading and enhance specific capacity and rate performance. Suppress manganese dissolution and enhance cycling stability Reversible migration and reutilization of Mn ²⁺	[79] [80] [86]
	CoSO ₄	Facilitate reversible redox reactions	[82]
	LiCl	Suppress zinc dendrite growth and stabilize the zinc anode	[87]
	CeCl ₃	Electrostatic shielding-induced uniform Zn deposition	[88]
	H ₂ SO ₄	Modulation of electrolyte acidity to inhibit zinc dendrite formation	[91]
	NHP	Stabilize the interfacial pH	[95]
	TiO ₂	Provide chemical adsorption sites and induce uniform Zn deposition	[102]
	SiO ₂	Lowering the nucleation energy barrier for zinc deposition	[104]
	Zn(BF ₄) ₂	Suppress zinc dendrite formation	[107]
Ionic Liquid	SO ₄ ²⁻	Promote uniform Zn ²⁺ diffusion and deposition	[110]
	EmimFSI	Mitigate the tip effect and regulate the SEI	[111]
	[BMIM]OTF	Enhances low-temperature tolerance and reduce zinc corrosion	[112]
Composite	(EMIM) ₅ Zn(OTf) ₂	Enhance low-temperature adaptability and adjust the solvation structure	[113]
	APA-NVO	Widen the operating voltage window and improve cycling stability	[117]
	EDA-VO	Facilitate ion transport and expand the ESW	[118]

number (29.8) compared to water (18), DMSO preferentially replaced water molecules in the Zn²⁺ solvation shell. This preferential solvation effect, coupled with strong DMSO–water interactions, jointly inhibited the decomposition of solvated water molecules. Moreover, decomposition products of solvated DMSO formed a SEI (Figure 10c,d) enriched with Zn₁₂(SO₄)₃Cl₃(OH)₁₅·5H₂O, ZnSO₃, and ZnS. This SEI not only prevented dendrite growth but also further suppressed water decomposition. Based on the ZnCl₂–H₂O–DMSO electrolyte, the Zn||Ti half cell achieved an average Coulombic efficiency of 99.5% over 400 cycles (400 h). Additionally, Zn||MnO₂ full cells with a low cathode/anode capacity ratio of 2:1 exhibited an energy density of 212 Wh kg⁻¹ (based on the total mass of both electrodes) and retained 95.3% of their capacity after 500 cycles at 8 C rate. Furthermore, Zhu et al.^[134] utilized pentaerythritol (PTT), a polyhydroxy alcohol, as an electrolyte additive. The four hydroxyl groups in its symmetric molecular structure effectively disrupted the hydrogen bond network in the conventional ZnSO₄ aqueous electrolyte, modifying the hydrogen bonding ratio among water molecules (Figure 10e–j) and altering the Zn²⁺

solvation structure. Both experimental and theoretical results demonstrated that PTT significantly suppressed water-induced side reactions and dendrite growth, thereby improving zinc reversibility and battery performance. The system exhibited an average Coulombic efficiency of 99.7% and a cycle stability exceeding 1000 h. In addition, the solvation structure of metal ions is a key factor affecting the occurrence of side reactions. The incorporation of chelating agents such as EDTA and citric acid, which form stable complexes with Zn²⁺, can effectively reduce direct interactions between free Zn²⁺ ions and water molecules. This suppresses Zn hydration-induced reduction reactions and mitigates hydrogen evolution and dendrite formation on the zinc anode, thereby enhancing cycling stability of Zn-based aqueous batteries.^[64,135–137] Moreover, certain trivalent inorganic metal ions such as La³⁺ and Al³⁺ can act as additives to regulate the hydration structure and coordination environment within the electrolyte, improving the system's overall resistance to decomposition.^[84,138] In summary, these additive strategies, from interfacial engineering to solution structure optimization, synergistically contribute to broadening the ESW of aqueous

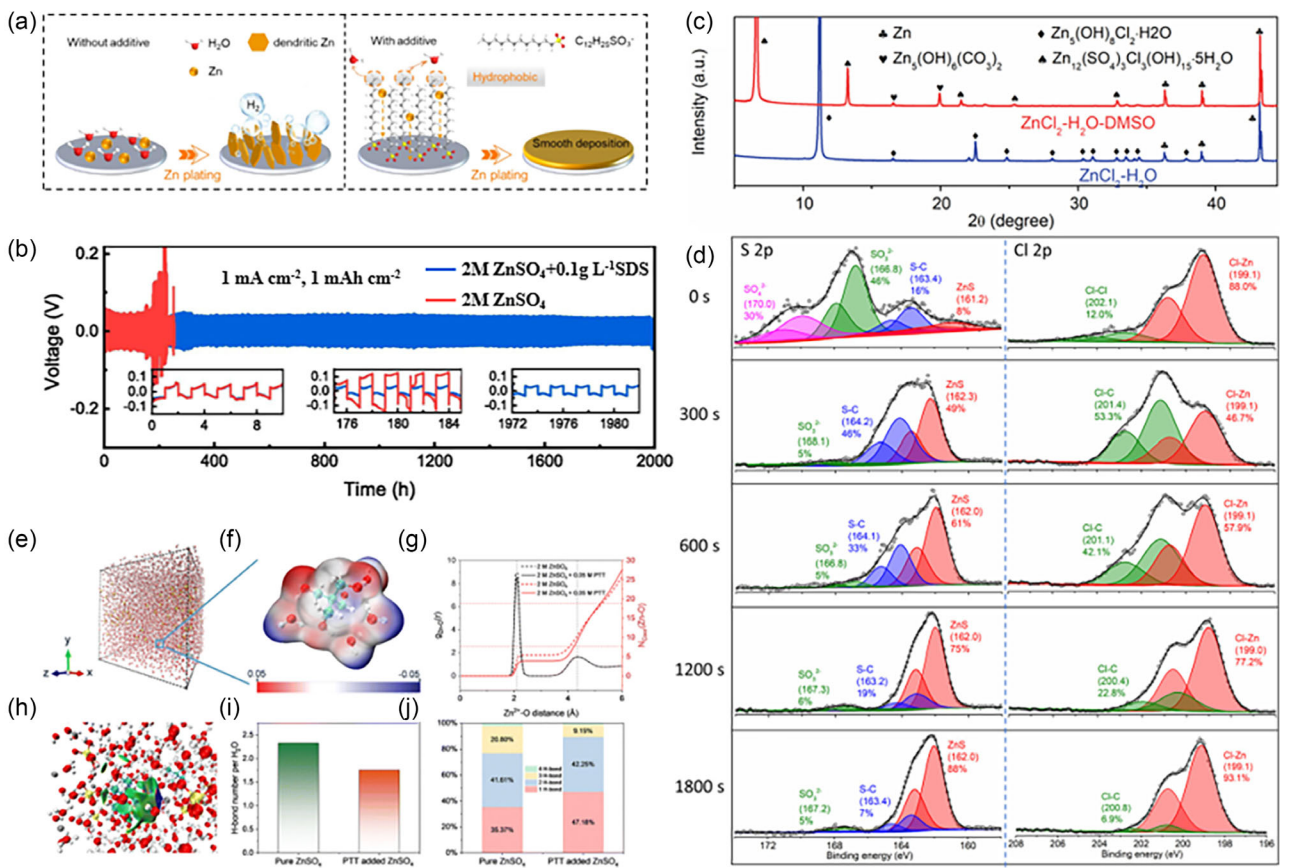


Figure 10. a) Schematic illustration of Zn surface evolution in electrolytes with and without the SDS additive. b) Voltage–time profiles of Zn symmetric cells operated at a current density of 1 mA cm^{-2} and a capacity of 1 mAh cm^{-2} .^[131] Reprinted from Journal of Colloid and Interface Science, Vol. 669, Fengyang Jing, Liangliang Xu, Yaru Shang, Gang Chen, Chade Lv, Chunshuang Yan, “Interface engineering enabled by sodium dodecyl sulfonate surfactant for stable Zn metal batteries,” Pages 984–991, Copyright (2024), with permission from Elsevier. c) X-ray diffraction patterns of Zn anodes after repeated plating/stripping cycles in $\text{ZnCl}_2\text{-H}_2\text{O-DMSO}$ and $\text{ZnCl}_2\text{-H}_2\text{O}$ electrolytes. d) XPS characterization of the SEI formed on Zn electrodes cycled in the $\text{ZnCl}_2\text{-H}_2\text{O-DMSO}$ electrolyte. The S 2p and Cl 2p spectra are presented with corresponding depth profiling results.^[132] Reprinted with permission from Longsheng Cao, Dan Li, Enyu Hu, Jijian Xu, Tao Deng, Lin Ma, Yi Wang, Xiao-Qing Yang, and Chunsheng Wang, “Solvation Structure Design for Aqueous Zn Metal Batteries,” J. Am. Chem. Soc., 2020, 142 (51), 21404–21409. Copyright 2020 American Chemical Society. Theoretical molecular dynamics (MD) simulations and analyses: e) Snapshot of the molecular model for pure ZnSO_4 electrolyte containing 0.05 M PTT additive. f) Electrostatic potential map of a PTT molecule coordinated with four water molecules. g) Coordination number (N_{coor}) and radial distribution function ($g(r)$) between Zn^{2+} and the first solvation shell in 2 M ZnSO_4 and 2 M ZnSO_4 with 0.05 M PTT, taken from the last 5 ns of equilibrium simulations. h) Snapshot showing intermolecular interactions between PTT and surrounding ZnSO_4 species in the 2 M ZnSO_4 + 0.05 M PTT system. i) Average number of hydrogen bonds (H-bonds) in the two electrolyte systems. j) Distribution of hydrogen bond types among water molecules in both systems. Color code: Red—O, White—H, Yellow—S, Cyan—C, Gray—Zn.^[134] Used with permission of Royal Society of Chemistry, from “Breaking hydrogen-bonds in aqueous electrolytes towards highly reversible zinc-ion batteries,” Yilong Zhu, Qianru Chen, Junnan Hao, and Yan Jiao, J. Mater. Chem. A, 2024, 12, 20097–20106; permission conveyed through Copyright Clearance Center, Inc.

electrolytes. They offer both theoretical insights and practical pathways for the development of high-performance AZIBs.

3.2. Suppression of Zinc Dendrite Growth

The growth of zinc dendrites remains one of the primary safety concerns in AZIBs.^[139–141] Due to the uneven deposition of zinc, dendrites can easily form and penetrate the separator, leading to internal short circuits. This not only poses serious safety hazards but also accelerates capacity fading and diminishes cycle life.^[142–144] To effectively suppress dendrite formation, researchers have proposed a variety of additive-based regulation strategies aimed at precisely controlling Zn^{2+} deposition behavior by tuning deposition kinetics, electric field distribution, and interfacial

structure. First, regulating the electric field distribution is considered a key factor in controlling Zn^{2+} migration and deposition direction. Certain organic additives with high dielectric constants can induce charge redistribution on the electrode surface, thereby homogenizing the local electric field. This reduces the tendency of Zn^{2+} to deposit rapidly at specific sites and inhibits dendrite nucleation.^[145,114] For instance, polyethylene glycol-200 (PEG-200), serving as a surfactant, can homogenize the interfacial electric field. In Zn-Zn symmetric cells, it yields a higher nucleation overpotential and a prolonged cycling stability of up to 890 h (compared to only 48 h for unmodified symmetric cells). Moreover, the electrode surface remains smooth after cycling, indicating successful dendrite suppression.^[146] Second, quasi-SEI forming additives can promote the formation of a compact

and uniform SEI layer on the zinc anode. This SEI layer forms through three primary mechanisms: decomposition, adsorption, and metal-ion coordination.^[19] The resulting interface layer guides Zn²⁺ to deposit in an ordered, planar manner, thereby forming dendrite-free layered structures and significantly improving deposition controllability. For example, Yin et al.^[147] introduced sodium 4-vinylbenzenesulfonate (VBS) as a multifunctional electrolyte additive. VBS spontaneously dissociates in water into Na⁺ and VBS⁻ anions. DFT calculations revealed that VBS⁻ exhibits strong adsorption affinity toward the Zn (002) facet, with an adsorption energy of -2.52 eV, significantly higher than that of water molecules. The differential charge density map indicates substantial electron cloud overlap between the sulfonate group and Zn atoms, confirming a stable chemisorption interaction. This preferential adsorption displaces interfacial water molecules and disrupts the hydrogen bonding network, resulting in the formation of an anion-rich and water-deficient EDL, which effectively suppresses hydrogen evolution and the formation of alkaline byproducts. Electrochemical impedance analyses further demonstrated that increasing VBS concentration leads to a decline in both differential capacitance and potential of zero charge, indicating a significant modulation of the EDL structure. Moreover, the $\text{—C}=\text{C}\text{—}$ moiety in the VBS molecule enables *in situ* electrochemical polymerization, forming a dense organic anionic SEI layer on the Zn surface (Figure 11a,b). The synergistic regulation of EDL and SEI notably enhances the interfacial stability and cycling performance of Zn||Zn symmetric cells, achieving a lifespan of over 1800 h at 1 mA cm⁻² and 1 mAh cm⁻². The introduction of VBS also improves the capacity retention and cycling stability of Zn|| δ -MnO₂ full cells. Zhang et al.^[148] introduced 1-butyl-3-methylimidazolium (BMIm⁺) as an electrolyte additive. This cation continuously induced preferential (002) crystal facet growth on the zinc electrode, effectively suppressing dendrite formation. Specifically, BMIm⁺ cations preferentially adsorbed onto the (100) and (101) facets of the zinc surface, thereby guiding Zn²⁺ deposition onto the (002) facet. This promoted a dense and flat deposition layer with preferential (002) orientation. Consequently, the zinc anode demonstrated long-term stability for up to 1000 h at a high current density of 10 mA cm⁻² and a capacity of 10 mAh cm⁻², with a Coulombic efficiency of 99.8%. Additionally, the NH₄V₄O₁₀||Zn pouch cell exhibited stable cycling over 240 cycles at 0.4 A g⁻¹ (Figure 11c-f). Furthermore, ion sieving effects have also shown promise in enabling uniform Zn deposition.^[149] Introducing multivalent inorganic cations with larger ionic radii can competitively occupy adsorption sites at the deposition interface, thereby preventing local Zn²⁺ accumulation and promoting broader, more uniform deposition. In one study, Mg²⁺ ions were found to suppress HER, enhance uniform Zn nucleation and deposition, and effectively inhibit dendrite formation. Compared to a baseline 2 M ZnSO₄ electrolyte, the Mg²⁺-modified electrolyte offered \approx 50% additional energy storage capacity and retained 98.7% capacity after 10,000 cycles.^[150] This improvement is attributed to the Mg²⁺-induced self-healing electrostatic shielding effect and regulation of the solvation sheath structure. Theoretical calculations further confirmed this mechanism (Figure 11g-i),

highlighting the critical role of electrolyte additives in achieving high energy density and long cycle life in ZIBs.

3.3. Enhancing Cycling Performance

The cycling performance of AZIBs is critically dependent on the reversibility of zinc anode deposition, the stability of the electrode/electrolyte interface, and the suppression of parasitic reactions.^[8,18] In conventional electrolyte systems, the zinc anode tends to form dendrites during cycling, leading to internal short circuits and capacity degradation. Additionally, side reactions such as hydrogen evolution and zinc corrosion significantly reduce the Coulombic efficiency and lifespan of the battery. In recent years, researchers have introduced functional electrolyte additives that effectively enhance the cycling performance of AZIBs by regulating ion migration, suppressing side reactions, and protecting electrode structures. First, certain additives can optimize the migration pathways of Zn²⁺ in the electrolyte, thereby reducing polarization and improving rate performance. For example, Qiu et al.^[151] proposed a novel additive strategy inspired by host-guest chemistry. They introduced the anion capturer β -cyclodextrin (β -CD) into Zn(ClO₄)₂ electrolyte to induce preferential Zn (002) deposition and improve Zn²⁺ migration behavior (Figure 11j). Their study demonstrated that ClO₄⁻ anions were captured within the β -CD cavity, reducing the Zn²⁺ migration energy barrier and significantly increasing the Zn²⁺ transference number to 0.878. Moreover, the β -CD@ClO₄⁻ complex guided the preferred growth of Zn crystals along the (002) plane, effectively inhibiting dendrite formation. As a result, compared to the pristine Zn(ClO₄)₂ electrolyte, the Zn||Zn symmetric cell exhibited a tenfold increase in cycle life, and the Zn-MnO₂ full cell showed a 57% capacity improvement at a current density of 0.1 A g⁻¹. Similarly, Wu et al.^[152] proposed a novel approach using biomass-derived cellulose nanocrystals (CNCs) as an electrolyte additive to address the issue of dendrite growth at the zinc anode. Benefiting from the self-assembly capability of CNCs under an electric field, this system enables dynamic interface reconstruction, significantly improving the interface stability. The self-healing behavior of CNCs occurs in a coordinated manner across different timescales: within seconds, CNCs rapidly migrate to high electric field regions; within minutes, the electrode voltage stabilizes; and within hours, a uniform protective layer is formed. Crosselectrolyte tests showed that, with the introduction of CNCs, the dendritic zinc anode could recover and maintain a cycling life of over 1000 h (Figure 12a). Scratch tests further demonstrated that the protective layer has excellent self-healing properties (Figure 12b). *In situ* Fourier Transform Infrared Spectroscopy (Figure 12c,d) and Raman spectroscopy (Figure 12e) revealed that CNCs regulate the Zn²⁺ solvation structure via —C—O—C groups, exhibiting periodic adsorption/desorption behavior in response to electric field reversals. Scanning electrochemical microscopy (SECM) results (Figure 12f) indicated that the local electric field becomes more uniform, with the probe current difference reduced to 0.50 nA. COMSOL simulations (Figure 12g,h) further confirmed that CNCs effectively redistribute

both the electric field and Zn^{2+} concentration field, promoting uniform electroplating/stripping. The developed CNCs-ZnSO₄ electrolyte system demonstrated an average Coulombic efficiency of 97.27% at 140 mA cm⁻² and stable cycling for over 980 h at a capacity of 50 mA h cm⁻². This strategy represents

a shift from static protection to dynamic, self-adaptive interface engineering, offering a promising new direction for the long-term stable operation of zinc-based energy storage systems. Moreover, Sun et al.^[153] reported a cost-effective additive—glucose—to modulate the traditional ZnSO₄ electrolyte system and improve

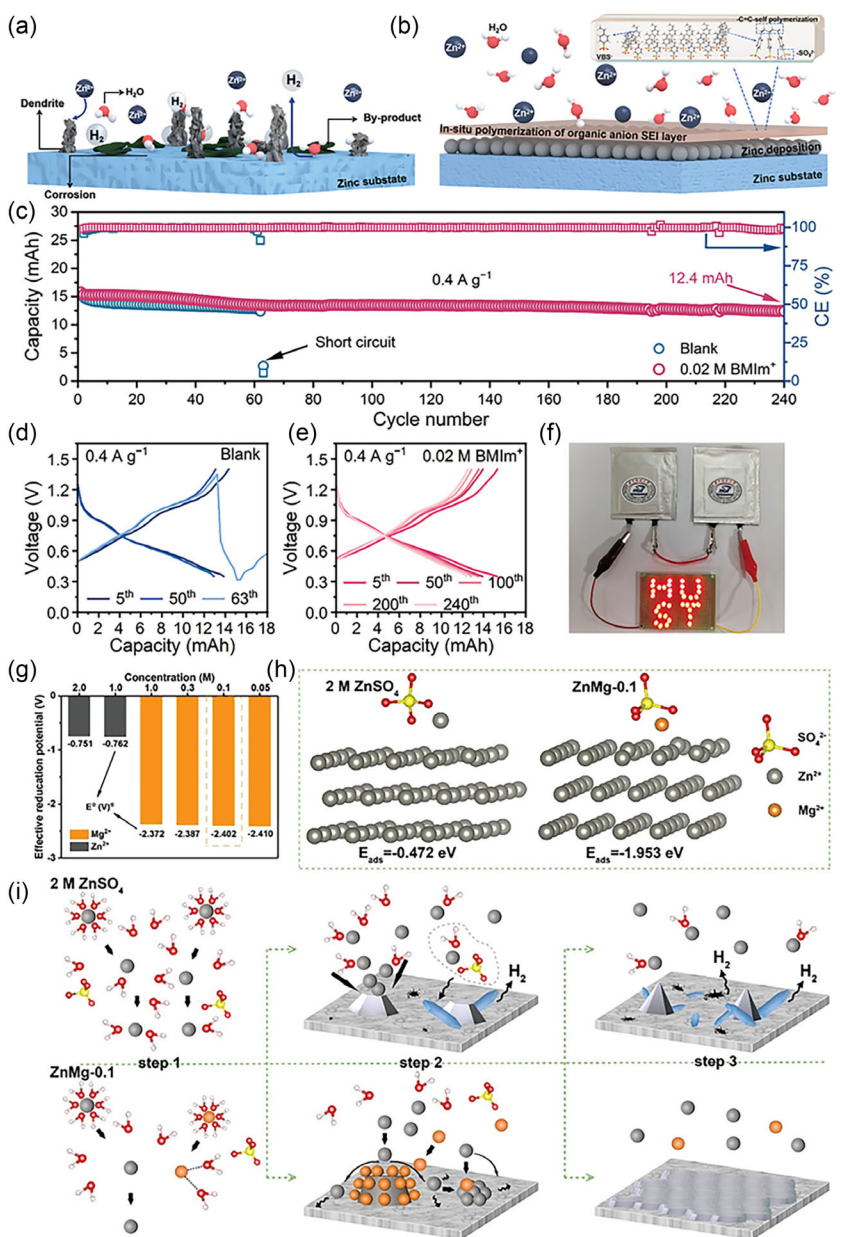


Figure 11. a,b) Schematic illustration of Zn deposition behavior in (a) ZnSO₄ and (b) VBS + ZnSO₄ electrolytes, highlighting the impact of the additive on deposition morphology. Reproduced with permission.^[147] Copyright (2024), Wiley-VCH. c) Long-term cycling performance of NH₄V₄O₁₀/Zn pouch cells operated in blank and 0.02 M BMIm-containing electrolytes at a current density of 0.4 A g⁻¹. d,e) Voltage profiles of the pouch cells at various cycles: (d) blank electrolyte and (e) 0.02 M BMIm electrolyte, both at 0.4 A g⁻¹. f) Digital image of two pouch cells connected in series using 0.02 M BMIm electrolyte to power light-emitting diodes, demonstrating practical applicability. Reproduced with permission.^[148] Copyright (2022), Wiley-VCH. g) Calculated effective reduction potentials of Zn²⁺ and Mg²⁺ at varying concentrations. h) Adsorption configurations and corresponding adsorption energies (E_{ads}) of electrolyte ions on the Zn surface, elucidating interfacial interactions. i) Schematic depiction of Zn deposition pathways in 2 M ZnSO₄ (top) and ZnMg-0.1 electrolytes (bottom), illustrating the role of Mg²⁺ in modulating deposition behavior. Reproduced with permission.^[150] Copyright (2021), Wiley-VCH. j) Comparison of ion transport mechanisms in Zn-MnO₂ full cells: conventional dual-ion transport in Zn(ClO₄)₂ electrolyte (left), and single-ion transport in Zn(ClO₄)₂- β -cyclodextrin (β -CD) complex electrolyte (right), highlighting the structural impact of host-guest chemistry on ion migration pathways. Reproduced with permission.^[151] Copyright (2022), Wiley-VCH.

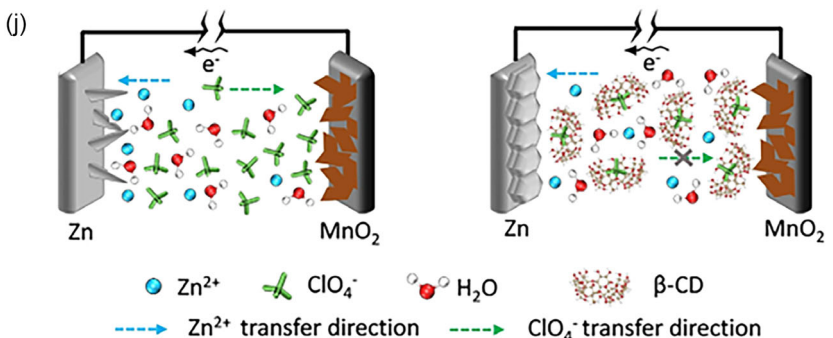


Figure 11. Continued.

the reversible plating/stripping of the zinc anode. In aqueous ZnSO_4 electrolytes, glucose regulated both the Zn^{2+} solvation structure and the zinc anode–electrolyte interface (Figure 13a,b). Specifically, glucose replaced one H_2O molecule in the $\text{Zn}^{2+}\text{-6H}_2\text{O}$ solvation shell, thereby suppressing parasitic reactions from active water decomposition. Glucose molecules also tended to adsorb onto the zinc anode surface, suppressing random dendrite growth. Second, electrolyte additives can also facilitate the formation of a stable SEI layer, effectively inhibiting side reactions. Liu et al.^[154] employed triethanolamine as an electrolyte additive to construct a hybrid solid–electrolyte interface composed of a static $\text{ZnSO}_4\text{-3Zn(OH)}_2\text{-4H}_2\text{O}$ layer and a dynamic quaternary ammonium ion adsorption layer. The static SEI served as a physical barrier between the zinc anode and electrolyte, preventing chemical corrosion and hydrogen evolution. The dynamic layer modulated interfacial ion flux and facilitated uniform Zn^{2+} deposition along the (002) orientation. Under a current density of 1.0 mA cm^{-2} and an areal capacity of 1.0 mA h cm^{-2} , the zinc anode exhibited a long cycling life of 2500 h and maintained a high Coulombic efficiency of 98.94%. Additionally, the $\text{Zn} \parallel \text{V}_2\text{O}_5$ full cell retained a high specific capacity of $178.4 \text{ mA h g}^{-1}$ after 500 cycles, demonstrating excellent capacity retention and cycling stability essential for practical applications. Furthermore, ammonium phytate has been utilized to form a Zn-rich protective layer on the anode, significantly enhancing reversibility. Xiao et al.^[155] introduced ammonium phytate as a multifunctional additive in traditional dilute ZnSO_4 electrolytes. The phytate anions, with their strong zinc affinity, formed a protective layer on the zinc surface that regulated the deposition process, mitigated parasitic reactions, and reduced harmful byproduct accumulation. Meanwhile, the competitive deposition between ammonium and Zn^{2+} ions promoted uniform zinc deposition, suppressing dendrite growth. As a result, the modified electrolyte exhibited outstanding performance, enabling Zn symmetric cells to cycle over 2000 h at 5 mA cm^{-2} and 1 mAh cm^{-2} with an average plating/stripping efficiency of 99.83% (Figure 13c). Lastly, certain additives interact directly with electrode materials to enhance structural stability. Materials such as PVP, lithium fluoride (LiF), and polyacrylonitrile (PAN) can form stable protective layers or modify the electrode surface structure, thereby enhancing electrode stability. These materials help prevent dissolution or structural collapse of active materials during

cycling, ultimately improving cycling stability and capacity retention. Thus, the introduction of functional additives has emerged as an effective strategy to improve the performance of AZIBs.

3.4. Enhancing Energy Density and Efficiency of AZIBs

AZIBs have garnered significant attention as next-generation energy storage systems owing to their inherent safety, low cost, and environmental friendliness. However, their energy density and energy efficiency remain constrained by several key factors, including a narrow ESW, poor reversibility of the zinc anode, and low utilization of electrode materials.^[89,141] In recent years, systematic research has focused on the design of functional electrolyte additives to modulate the electrolyte system at the molecular level. These efforts aim to achieve multidimensional improvements in battery performance, particularly in extending the voltage window, enhancing zinc deposition/stripping efficiency, suppressing side reactions, and prolonging cycling life. The narrow ESW in traditional aqueous systems arises from the thermodynamic decomposition voltage of water ($\approx 1.23 \text{ V}$), which limits the stable operation of high-voltage cathode materials. To address this, researchers have developed strategies to tune Zn^{2+} solvation structures and reduce water activity, thereby effectively suppressing HER. For example, Leng et al.^[156] introduced 1-ethyl-3-methylimidazolium dicyanamide ([Emim][DCA], or ED) into the electrolyte, successfully inhibiting water reduction and zinc dendrite growth. The strong coordination between zinc and nitrogen-containing ligands facilitates the adsorption of DCA⁻ anions on the zinc anode surface, forming a dense $\text{Zn}(\text{DCA})_2$ protective layer. This layer not only promotes Zn^{2+} desolvation but also isolates water molecules, enabling zinc deposition under quasiwater-free conditions and enhancing plating/stripping reversibility. Additionally, in water-deficient electric double-layer environments, Zn^{2+} can direct triflate anions to migrate toward the zinc electrode surface, forming an *in situ* fluorine-based SEI. This SEI effectively isolates the zinc electrode from water, thereby suppressing corrosion and HER. As a result, the $\text{Zn}||\text{Zn}$ symmetric cell exhibited over 2500 h of cycling at 0.5 mA cm^{-2} and 0.5 mA h cm^{-2} , while the $\text{Zn}||\text{Ti}$ asymmetric cell achieved a Coulombic efficiency of 99.4%. The $\text{Zn}||\text{PANI}$ full cell maintained capacity stability after 1000 cycles (Figure 13d) at a

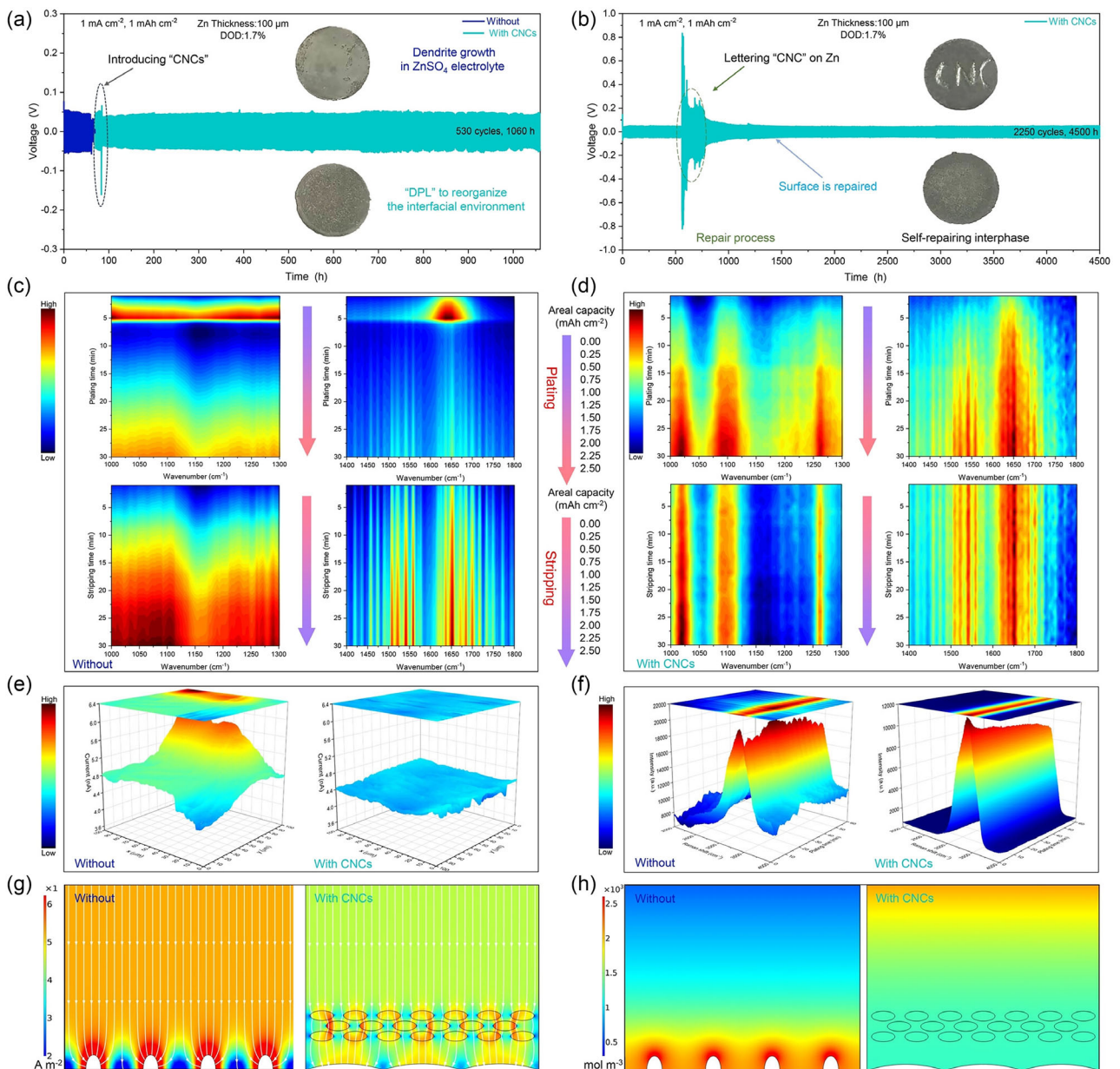


Figure 12. Validation of dynamic interfaces for real-time protection of zinc chemical systems. a) Voltage profiles of Zn||Zn symmetrical cells cycling in ZnSO₄ electrolyte for the first 35 cycles, followed by the introduction of CNCs under 1 mA cm⁻², 1 mAh cm⁻². b) Cycling performance of Zn||Zn symmetrical cells in CNCs-ZnSO₄ electrolyte before and after lettering recombination under 1 mA cm⁻², 1 mAh cm⁻². In situ FTIR spectra of the Zn plating/stripping process in the central region of the ZnSO₄ electrolyte: c) without CNCs and d) with CNCs at 5 mA cm⁻² for 30 min. e) The change in feedback current, obtained via SECM area scans with feedback mode, on the cycled Zn anode surface under 50 mA cm⁻², 50 mAh cm⁻² in ZnSO₄ electrolyte with/without CNCs. f) In situ Raman spectra of v-O-H based on symmetrical cells in ZnSO₄ electrolyte with/without CNCs. Simulated electric field distributions: g) and Zn²⁺ concentration field distributions h) during the Zn deposition process on the Zn electrode with/without CNCs. Reproduced with permission.^[152] Copyright (2024), Wiley-VCH.

current density of 4 A g⁻¹. In another study, Liu et al.^[157] introduced the flame-retardant triethyl phosphate (TEP) as a cosolvent with strong solvation capability. TEP, with a higher donor number (26 kcal mol⁻¹) than H₂O (18 kcal mol⁻¹), preferentially forms TEP-dominated inner solvation shells around Zn²⁺ and forms strong hydrogen bonds with water. This TEP-coordinated electrolyte structure inhibits side reactions between H₂O and V₂O₅, while enabling the in situ formation of a stable polymer-inorganic hybrid phase (poly-ZnP₂O₆ and ZnF₂) on the zinc anode, which

suppresses dendrite growth and parasitic water reactions. Under this optimized electrolyte system, the Zn||Cu cell demonstrated an average Coulombic efficiency of up to 99.5%. A full cell with a low Zn: V₂O₅ capacity ratio (2:1) and lean electrolyte conditions (11.5 g Ah⁻¹) maintained a reversible capacity of ≈250 mA h g⁻¹ after over 1000 cycles at 5 A g⁻¹. To address issues of low electrode utilization and dendrite formation, interfacial-regulating additives have also become a research focus. Xie et al.^[158] introduced taurine, a zwitterionic additive with

an isoelectric point, and developed an environment-adaptive interfacial strategy to enhance zinc anode stability. Taurine adjusts its net charge based on local conditions and chelates with Zn^{2+} under alkaline environments, forming an in situ

hydrophobic and zincophilic protective layer that buffers pH fluctuations and suppresses hydrogen evolution and dendrite growth. Experimental and theoretical results confirmed that the taurine-derived layer improves ion distribution and promotes

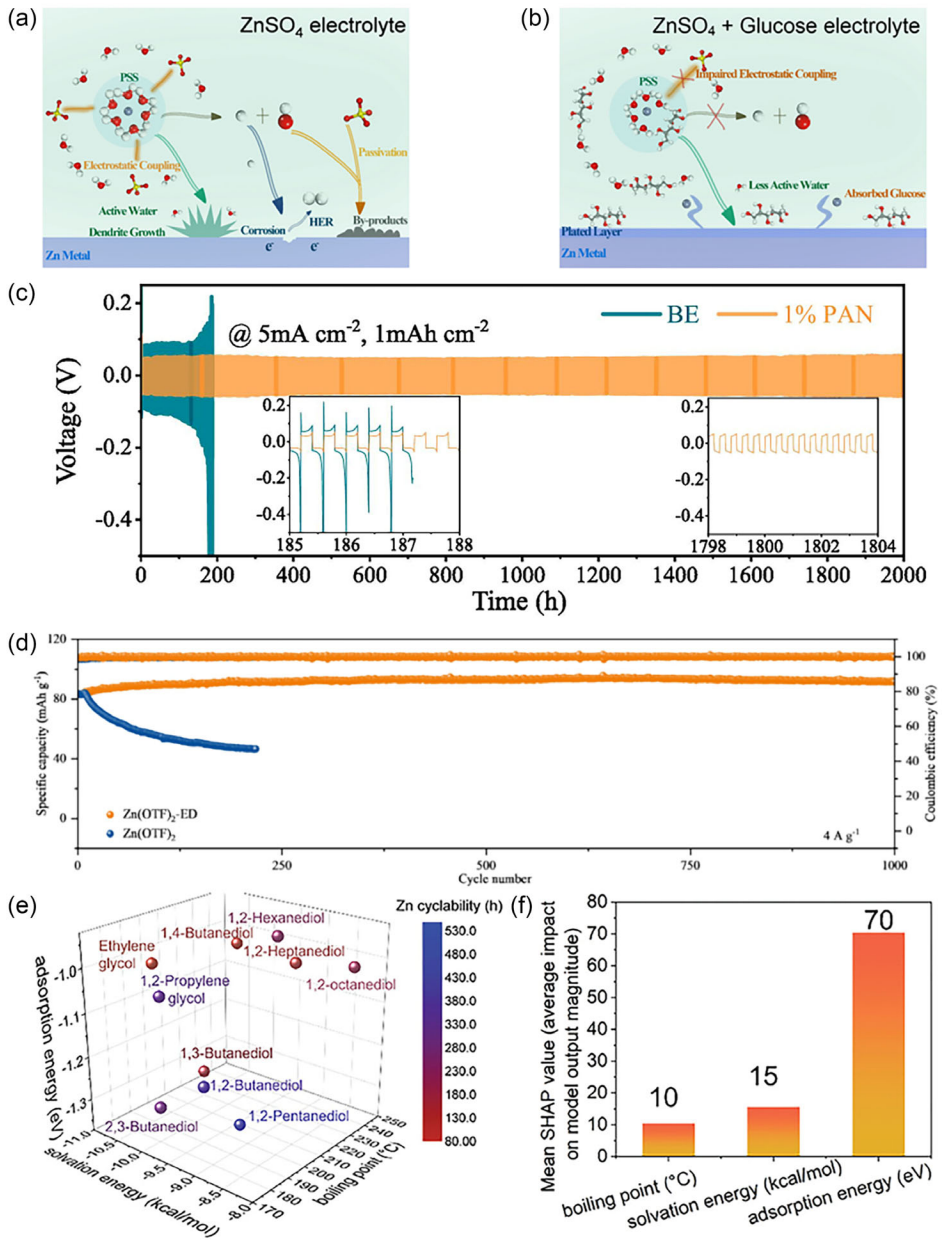


Figure 13. Schemes illustrating different reaction processes of Zn^{2+} solvation structure and corresponding interfacial interaction between Zn anode surface and electrolyte under a) $ZnSO_4$ and b) $ZnSO_4$ -glucose electrolytes. Reproduced with permission.^[153] Copyright (2021), Wiley-VCH. c) Cycling performance of $Zn||Zn$ symmetric battery at 5 mA cm^{-2} and 1 mAh cm^{-2} .^[155] Reprinted from Chemical Engineering Journal, Vol. 489, Fangyuan Xiao, Xiaoke Wang, Kaitong Sun, Qian Zhao, Cuiping Han, and Hai-Feng Li, "Zincophilic armor: Phytate ammonium as a multifunctional additive for enhanced performance in aqueous zinc-ion batteries," Article No. 151111, Copyright (2024), with permission from Elsevier. d) Long-term cycling performance of the $Zn||PANI$ cell in $Zn(OTF)_2$ and $Zn(OTF)_2$ -ED electrolyte at 4 A g^{-1} .^[156] Reprinted from Journal of Energy Storage, Vol. 121, Jiaqi Leng, Xiaofang Wang, Dan Li, Ruru Shi, Xingyun Zhu, Longsheng Cao, and Qingda An, "Engineering coordination interactions and conversion layers for enhanced performance of aqueous zinc ion batteries," Article No. 116502, Copyright (2025), with permission from Elsevier. Machine learning-based rationalization of the additive performance. e) The alkanediol additive performance mapped in the parameter space defined by three performance descriptors, the adsorption energy of the additive on zinc, the additive solvation energy (additive-water interaction), and the additive association energy represented by the additive boiling point. f) Machine learning-based correlation of the performance with the three performance descriptors. Machine learning-based SHapley Additive exPlanations analysis of the cycling performance relative to g) the additive solvation energy and h) the additive adsorption energy. Reproduced with permission.^[159] Copyright (2023), with permission from the Authors (Advanced Materials published by Wiley-VCH GmbH).

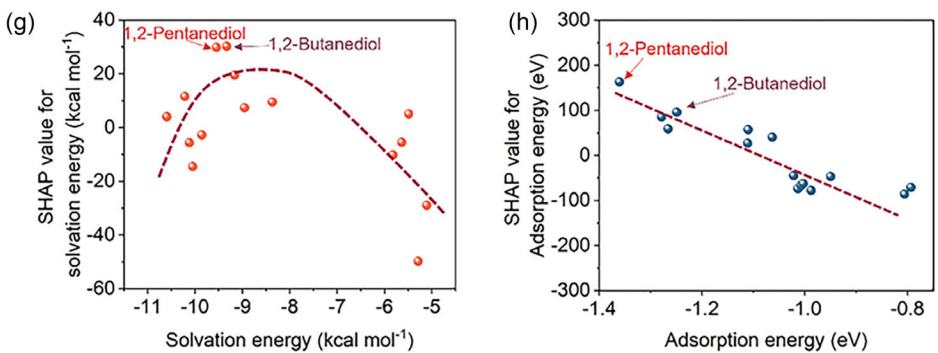


Figure 13. Continued.

uniform, reversible zinc deposition. Under 5 mA cm⁻²/5 mAh cm⁻² cycling, Zn||Zn cells remained stable for over 1800 h, while NH₄V₄O₁₀ full cells retained 89.8% capacity after 1200 cycles, indicating excellent long-term performance. Moreover, AI-assisted screening technologies have recently been applied to additive development. Shang et al.^[159] screened various alcohols and glycols, identifying 1,2-butanediol and pentanediol as highly effective additives for the zinc anode. Even at low concentrations (1 vol%), these additives form dynamic SEIs with strong interfacial film-forming capabilities, effectively suppressing corrosion and dendrite growth, extending zinc anode lifespan by 5–20 times, and achieving a Coulombic efficiency of 99.9%. These additives also enhanced performance under harsh conditions such as high temperature. Notably, machine learning methods (Figure 13e–h) revealed intrinsic correlations between zinc cycling performance and physicochemical descriptors of the additives (e.g., adsorption energy, solubility, binding energy), deepening understanding of additive mechanisms and offering valuable insights for the rational design of high-performance electrolyte additives. In terms of overall energy efficiency improvement, the development of bifunctional or multifunctional additives has also shown great promise. Li et al.^[160] introduced a dual-additive system combining zinc acetate (Zn(OAc)₂) and trimethylamine N-oxide (TMAOAc), serving as pH buffer and electrostatic shield respectively, achieving nearly 100% Coulombic efficiency and over 3600 h of cycling stability.

Recently, Cao et al.^[161] developed a multifunctional additive, sodium 2,4-disulfonate benzaldehyde (B24DADS), designed to modulate Zn²⁺ solvation structures and form passive SEI layers on the zinc anode surface to suppress dendrite growth and side reactions. Through synergistic effects of induced deposition, SEI formation, and texture modulation, uniform zinc deposition was achieved. Under critical conditions (20 mA cm⁻²/20 mA h cm⁻²), the zinc anode exhibited outstanding cycling performance of up to 3700 h with a low polarization voltage (0.02 V). Interestingly, Zhang et al.^[162] introduced cyclodextrins (CDs) as supramolecular agents to modulate Zn²⁺ solvation structures via host-guest coordination chemistry. This strategy effectively suppressed side reactions, broadened the ESW, promoted uniform zinc deposition, and refined crystal grain size, significantly enhancing anode stability. Among them, γ -CD, due to its strongest interaction with

Zn²⁺, exhibited superior performance over α -CD and β -CD. The γ -CD-assisted Zn||Zn symmetric battery demonstrated over 2400 h of stable cycling at a current density of 1 mA cm⁻², showcasing the great potential of supramolecular strategies for constructing high-performance zinc anodes.

4. Influence of Electrolyte Additives on the Performance of AZIBs

AZIBs are emerging as promising candidates for next-generation energy storage systems. However, they face several performance challenges, particularly in terms of battery efficiency, cycling stability, and safety.^[163] Electrolyte additives, as a critical component for optimizing battery performance, can significantly enhance various aspects of ZIBs. This section provides a detailed overview of how electrolyte additives influence ZIB performance, with an emphasis on their effects on efficiency, cycling stability, and safety.

4.1. Impact on Battery Efficiency

Battery efficiency, one of the core metrics for evaluating battery performance, generally includes parameters such as coulombic efficiency, energy density, and power density. Electrolyte additives improve ZIB efficiency by modifying the physicochemical properties of the electrolyte. The primary mechanisms involve enhancing Zn²⁺ ion mobility, optimizing the interfacial reactions between electrolyte and electrodes, and expanding the ESW of the electrolyte. Yang et al.^[164] reported the use of 3-(hydroxy(phenyl)phosphinyl)propanoic acid (HPA) as an electrolyte additive. Leveraging its amphiphilic functional groups and multiple coordination sites, HPA formed a micellar network structure within the aqueous electrolyte, enabling directional adsorption and transport of Zn²⁺ ions and acting as an ionic flux stabilizer. Furthermore, strong adsorption of HPA on the zinc surface induced the in situ formation of an organic-inorganic hybrid SEI, which effectively enhanced charge transfer kinetics and suppressed interfacial side reactions. At a current density of 4 mA cm⁻², the additive achieved an average Zn plating/stripping efficiency of 99.91% and maintained excellent reversibility even

at 120 mA cm^{-2} . After 7 days of calendar aging, the initial Coulombic efficiency of Zn||Cu cells reached 71.74%, significantly higher than 42.59% for the control group. The Zn||MnO₂ full cell retained 80% of its capacity after 1100 cycles at 2 A g^{-1} , compared to only 37% in the control group. This study revealed the molecular-level regulation mechanism of the electrolyte network structure and its influence on interfacial/interphase dynamics, offering theoretical guidance for the development of efficient and durable zinc-metal batteries and other metal anode systems. In addition, inorganic metal salts have also proven effective as electrolyte additives. These salts enhance ionic conductivity, facilitate Zn²⁺ migration, and reduce internal resistance during charge/discharge processes. This improvement leads to decreased energy loss and significantly increased charge/discharge efficiency, especially under high-rate and long-term cycling conditions. Moreover, metal salts can modulate the physicochemical properties of the electrolyte, thereby broadening its ESW. This expansion not only suppresses water decomposition reactions but also stabilizes battery performance under diverse operating conditions. Preventing water electrolysis at high voltages avoids gas accumulation and Zn dendrite growth, both of which can compromise cycling stability and safety. Thus, the addition of metal salts improves chemical stability and supports high-performance battery operation under elevated voltage and temperature conditions.

4.2. Impact on Cycling Stability

Cycling stability, which reflects a battery's service life, is crucial for long-term performance. Electrolyte additives contribute to cycling stability by various means, especially by suppressing zinc dendrite growth and improving the uniformity of Zn deposition on the anode surface. Zinc dendrites not only degrade efficiency but also pose safety risks such as short-circuiting and thermal runaway. Xu et al.^[140] introduced a small amount (2 vol%) of diethyl ether (Et₂O) as an additive in the electrolyte, significantly improving the electrochemical performance of Zn–MnO₂ batteries. The presence of Et₂O led to a first-cycle Coulombic efficiency of 95.6% at 50 mA g^{-1} , and even under high-rate conditions of 5 A g^{-1} , the battery delivered a discharge capacity of $115.9 \text{ mA h g}^{-1}$. After 4000 cycles, the capacity retention reached an impressive 97.7%, which ranks among the best for Mn-based ZIBs in mild electrolytes. Ex situ analyses revealed that the inclusion of Et₂O effectively suppressed Zn dendrite formation, which was the key factor in enhancing cycling stability. Furthermore, fluoride compounds and lithium salts are also effective in inhibiting dendrite growth.^[87] Fluoride additives, for instance, can form a protective layer on the zinc anode, preventing irregular Zn²⁺ deposition and thus extending cycle life.^[165] These protective films not only reduce dendrite formation but also enhance the chemical stability of the electrolyte. Calcium-based compounds can further promote uniform Zn deposition and reduce surface roughness, leading to improved cycle stability. Studies have shown that Zn–Ca complexes as additives significantly enhance capacity retention and extend the overall cycle life.^[166]

4.3. Impact on Safety

Safety is a critical factor for the commercial application of ZIBs, particularly concerning overcharging, thermal runaway, and electrolyte leakage.^[167,168] Electrolyte additives can improve safety, enabling stable operation under harsh conditions. Overcharging, a major cause of battery failure, can be mitigated by certain inorganic additives such as aluminum and sodium salts.^[169] Zhou et al.^[84] developed a novel mixed electrolyte incorporating Al³⁺ ions. The presence of Al³⁺ drastically reduced insulating zinc salt formation on the cathode surface and expanded the electrochemical voltage window from 3.0 to 4.35 V. Notably, Al³⁺ doping also enhanced crystal structure stability and suppressed dendrite growth. In this system, Zn||Zn symmetric cells achieved a remarkable cycle life of 1500 h at 3 mA cm^{-2} , while Zn||KVO full cells maintained 91% capacity retention over 1600 h at 100 mA g^{-1} . Yang et al.^[170] introduced bromine-containing additives (tetrabutylammonium and benzyl trimethylammonium bromide), creating a self-sacrificial electrolyte. These additives preferentially underwent oxidation before electrolyte decomposition, forming a Br⁻/Br₂ redox pair that stabilized the chemical environment.^[11] This strategy ensured prolonged overcharge protection: even at 200% state of charge, Zn||MnVO and Zn||MnO₂ batteries operated stably for over 650 and 550 h, respectively. Thermal stability of the additives also plays a vital role in safety. Wang et al.^[171] introduced diethylene glycol monomethyl ether (DG) as an electrolyte additive, which significantly enhanced the electrochemical performance of zinc anodes across a wide temperature range (-35 to 65°C). DG disrupts the hydrogen bond network in aqueous electrolytes, reconstructs the Zn²⁺ solvation shell, suppresses hydrogen evolution and corrosion, and simultaneously lowers the freezing point, thereby broadening the operating temperature window. In situ EQCM-D and XPS analyses revealed that DG–OTF⁻ complexes undergo reductive decomposition during cycling, forming a composite SEI layer composed of ZnF₂ and ZnS, which effectively mitigates side reactions and promotes uniform Zn deposition. Electrochemical tests demonstrated that Zn||Zn symmetric cells with DG exhibited a long cycling life of up to 3500 h at 25°C (1 mA cm^{-2}) and remained stable for over 1000 h under extreme temperatures (-35 and 65°C). In Zn||Cu cells operated at 65°C , the DG-containing electrolyte (40 vol%, DG40) enabled stable cycling for 800 h, in stark contrast to the control group without DG (DG0), which failed after only 30 h. Furthermore, the DG40 system maintained a high Coulombic efficiency (CE) of 99.2% after 800 cycles, while DG0 exhibited a low initial CE of only 44.9%. These findings underscore the effectiveness of DG in regulating Zn²⁺ solvation, stabilizing the electrode–electrolyte interface, and suppressing parasitic reactions, especially under high-temperature conditions. ILs can enhance both conductivity and thermal stability of the electrolyte. Li et al.^[44] synthesized triazole-based ILs (T1, T2, and T3) using Cu(I)-catalyzed azide–alkyne click chemistry. The hydroxyl group content influenced their physicochemical properties: fewer hydroxyl groups resulted in improved stability and ionic conductivity. The T1, T2, and T3 exhibited ESWs of 4.76, 4.11, and 3.52 V, respectively. When Zn(CF₃SO₃)₂ and LiTFSI were

added to T1, the conductivity increased to 1.55×10^{-3} S cm $^{-1}$ and the ESW to 6.36 V. Batteries based on the T1S-20 electrolyte delivered an initial capacity of 81 mA h g $^{-1}$ at 30 °C, retaining 89% after 50 cycles. At 80 °C, the capacity increased to 111 mA h g $^{-1}$ with 93.6% retention after 100 cycles. Compared to aqueous electrolytes (71.8% retention), T1S-20 showed superior high-temperature performance. Zhang et al.^[172] incorporated silk fibroin (SF) as a multifunctional additive in a ZnCl₂-based “water-in-salt” electrolyte system. SF improved electrolyte structure and regulated electrode interfacial behavior. In Zn||Zn half cells, the system exhibited excellent interfacial stability, with a low polarization voltage of 180 mV at 1 mA cm $^{-2}$ and stable operation for over 200 h at 2 mA cm $^{-2}$ and 60 °C. Mechanistic studies showed that SF disrupted hydrogen bonding networks among H₂O molecules and Zn²⁺ coordination, reducing viscosity, enhancing ion mobility, and suppressing side reactions. Moreover, SF enabled *in situ* formation of hydrophilic/zincophilic interfacial films, promoting uniform Zn deposition, suppressing dendrite formation, and stabilizing the cathode structure. In practical tests, Zn||V₂O₅ nH₂O pouch cells delivered \approx 72 Wh L $^{-1}$ energy density and operated stably from -60 to 60 °C. Finally, some organic additives can reduce electrolyte viscosity, thereby lowering leakage risks and further enhancing overall battery safety.

5. Conclusion and Outlook

AZIBs have garnered significant attention in recent years for application in renewable energy storage systems, owing to their inherent safety, abundant material availability, low manufacturing costs, and environmental friendliness. However, the presence of side reactions in the electrolyte system—such as hydrogen evolution, zinc dendrite growth, and anode corrosion—severely limits the energy efficiency, cycle life, and practical viability of AZIBs. As an effective approach to modulate electrolyte properties and interfacial reactions, electrolyte additives have demonstrated remarkable potential and broad prospects for enhancing the overall performance of AZIBs.

This review systematically examined the application of electrolyte additives in AZIBs, including their classification, mechanisms of action, impact on battery performance, recent research progress, and future directions. First, from the perspective of additive types, we introduced various functional categories—such as organic additives (e.g., surfactants, corrosion inhibitors, chelating agents), inorganic additives (e.g., metal ions, acids/bases, salts), ILs, and organic–inorganic composite additives—and their differentiated roles in tuning electrolyte composition and the zinc anode/electrolyte interfacial behavior. Then, from a mechanistic standpoint, we discussed the core functions of additives in suppressing zinc dendrite growth, expanding the ESW, improving ion transport behavior, and constructing stable SEIs. In terms of performance enhancement, additives have been shown to significantly improve the energy and power densities of AZIBs, extend their cycling lifespan, and enhance both thermal stability and operational safety. Furthermore, recent studies suggest a growing research trend toward multifunctional composite

additives, as well as the development of green, stable, and low-cost additive materials.

Despite the considerable progress made at the experimental level, electrolyte additives still face several challenges in practical applications. Future research should focus on the following key areas.

5.1. Establishing a Theory-Guided and Data-Driven Design Framework for Electrolyte Additives

The current development of electrolyte additives still relies heavily on empirical trial-and-error approaches, which are inefficient and lack predictive insight into structure–performance relationships. Future research should integrate DFT, MD, and other theoretical modeling tools to establish models of additive–Zn interface interactions. Coupled with high-throughput screening and machine learning algorithms, a closed-loop system involving theoretical calculation–data analysis–experimental validation should be established to enhance design precision and development efficiency.

5.2. Developing Multifunctional Composite Additives for Synergistic Interface Regulation

To address multiple challenges under practical working conditions, it is imperative to design integrated additives with multifunctionality, such as dendrite suppression, corrosion mitigation, interfacial stabilization, and SEI formation. Strategies involving organic–inorganic hybridization, surfactant–nanoparticle synergy, or molecular self-assembly can be employed to modulate Zn²⁺ solvation structures and improve interfacial stability. A coordinated design of structure and function will be key to unlocking the full potential of composite additives.

5.3. Enhancing Practical Evaluation and Engineering Feasibility of Additives

Most current studies are conducted under idealized laboratory conditions and fail to reflect real-world operating scenarios. Future efforts should prioritize systematic evaluation of additive performance under high areal loading (>5 mg cm $^{-2}$), high current density (>5 mA cm $^{-2}$), and wide temperature ranges (-20 to 60 °C). Additionally, attention should be paid to the additives’ compatibility with full-cell systems, including ionic conductivity, pH stability, and suppression of side reactions. Scalable synthesis, safety, and cost-effectiveness will be critical for industrial application.

5.4. Pursuing Green and Sustainable Development of Additive Materials

While AZIBs offer intrinsic safety and environmental advantages, the use of toxic or nondegradable additives may compromise these benefits. Future research should emphasize the development of green additives derived from natural, biodegradable,

and lowtoxicity sources, such as amino acids, polysaccharides, and plant extracts. The life-cycle environmental impact, particularly the nature of degradation byproducts after long-term cycling, should be thoroughly assessed to ensure both electrochemical performance and ecological sustainability.

5.5. Establishing Standardized Evaluation Protocols and Open-Access Databases to Enable Intelligent Screening

The lack of standardized testing methods and comparable metrics currently hampers meaningful progress in additive research. It is imperative to construct a comprehensive evaluation framework encompassing electrochemical performance (e.g., cycling life, Coulombic efficiency, ionic conductivity), interfacial behavior (e.g., SEI formation, hydrogen evolution suppression), thermal stability, and environmental impact. An open-access database that integrates additive structures, properties, and synthesis protocols will support AI-assisted screening, promote data sharing, and accelerate the discovery and deployment of high-performance electrolyte additives.

In conclusion, electrolyte additives play an irreplaceable and central role in the optimization of AZIBs. They serve as a crucial link between fundamental research and practical application. Through interdisciplinary collaboration, the integration of theoretical and experimental studies, and joint efforts across the entire industrial chain, it is expected that current technical bottlenecks will be overcome. These advancements will pave the way for AZIBs to achieve higher energy density, longer cycle life, improved safety, and greater practical viability, thereby contributing strong support to the development of global green energy storage systems.

Acknowledgements

This work was supported by the National Natural Science Foundation of China (21606051, 22278276) and the Natural Science Foundation of Guangdong Province (2022A1515010205).

Conflict of Interest

The authors declare no conflict of interest.

Keywords: electrolyte additive • hydrogen evolution • solid electrolyte interphase protection layer • solvation structure • zinc dendrite • zinc-ion batteries

- [1] H. Togun, A. Basem, T. Abdulrazzaq, N. Biswas, A. M. Abed, J. M. dhabab, A. Chattopadhyay, K. Slimi, D. Paul, P. Barmavatu, A. Chrouda, *Appl. Energy* **2025**, 388, 125726.
- [2] C. Zhang, S. Chou, Z. Guo, S.-X. Dou, *Adv. Funct. Mater.* **2024**, 34, 2308001.
- [3] Y. Wu, H. Ye, Y. Li, *Adv. Funct. Mater.* **2025**, n/a, 2424329.
- [4] M. Li, J. Lu, Z. Chen, K. Amine, *Adv. Mater.* **2018**, 30, 1800561.
- [5] S.-T. Myung, Y.-K. Sun, *Chem. Soc. Rev.* **2017**, 46, 3529.
- [6] S. Dhir, S. Wheeler, I. Capone, M. Pasta, *Chem* **2020**, 6, 2442.
- [7] A. Ponrouch, C. Frontera, F. Bardé, M. R. Palacín, *Nat. Mater.* **2016**, 15, 169.

- [8] G. Fang, J. Zhou, A. Pan, S. Liang, *ACS Energy Lett.* **2018**, 3, 2480.
- [9] M. Tang, Q. Liu, X. Zou, B. Zhang, L. An, *Adv. Mater.* **2025**, n/a, 2501361.
- [10] Z. Yi, G. Chen, F. Hou, L. Wang, J. Liang, *Adv. Energy Mater.* **2021**, 11, 2003065.
- [11] Y. Zhu, G. Liang, X. Cui, X. Liu, H. Zhong, C. Zhi, Y. Yang, *Energy Environ. Sci.* **2024**, 17, 369.
- [12] J. Wei, P. Zhang, J. Sun, Y. Liu, F. Li, H. Xu, R. Ye, Z. Tie, L. Sun, Z. Jin, *Chem. Soc. Rev.* **2024**, 53, 10335.
- [13] Z. Xu, Y. Sun, J. Xie, S. Liu, Y. Nie, X. Xu, J. Tu, F. Chen, T. Zhu, X. Zhao, *ACS Sustain. Chem. Eng.* **2023**, 11, 14176.
- [14] M. Iturroundobeitia, O. Akizu-Gardoki, O. Amondarain, R. Minguez, E. Lizundia, *Adv. Sustainable Syst.* **2022**, 6, 2100308.
- [15] Z. Guo, Y. Ma, X. Dong, J. Huang, Y. Wang, Y. Xia, *Angew. Chem. Int. Ed.* **2018**, 57, 11737.
- [16] L. E. Blanc, D. Kundu, L. F. Nazar, *Joule* **2020**, 4, 771.
- [17] L. Kang, M. Cui, Z. Zhang, F. Jiang, *Batteries Supercaps* **2020**, 3, 966.
- [18] F. Wang, O. Borodin, T. Gao, X. Fan, W. Sun, F. Han, A. Faraone, J. A. Dura, K. Xu, C. Wang, *Nat. Mater.* **2018**, 17, 543.
- [19] Z. Wu, Z. Huang, R. Zhang, Y. Hou, C. Zhi, *Int. J. Extreme Manuf.* **2024**, 6, 062002.
- [20] S. Xie, X. Li, Y. Li, Q. Liang, L. Dong, *Chem. Rec.* **2022**, 22, e202200201.
- [21] N. Zhang, J.-C. Wang, Y.-F. Guo, P.-F. Wang, Y.-R. Zhu, T.-F. Yi, *Coord. Chem. Rev.* **2023**, 479, 215009.
- [22] X. Chen, H. Zhang, J.-H. Liu, Y. Gao, X. Cao, C. Zhan, Y. Wang, S. Wang, S.-L. Chou, S.-X. Dou, *Energy Storage Mater.* **2022**, 50, 21.
- [23] T. Lv, Y. Peng, G. Zhang, S. Jiang, Z. Yang, S. Yang, H. Pang, *Adv. Sci.* **2023**, 10, 2206907.
- [24] J. Liu, Z. Shen, C.-Z. Lu, *J. Mater. Chem. A* **2024**, 12, 2647.
- [25] L.-L. Zhao, Y.-H. Zhao, Y.-M. Wu, P.-F. Wang, Z.-L. Liu, Q.-Y. Zhang, J. Shu, T.-F. Yi, *Energy Storage Mater.* **2025**, 78, 104299.
- [26] H. Zhang, X. Liu, X. Chen, B. Yang, Y. Lu, Q. Jiang, Q. Liu, *J. Energy Storage* **2024**, 78, 110326.
- [27] L. Lin, Z. Lin, J. Zhu, K. Wang, W. Wu, T. Qiu, X. Sun, *Energy Environ. Sci.* **2023**, 16, 89.
- [28] X. Guo, G. He, *J. Mater. Chem. A* **2023**, 11, 11987.
- [29] Y. Zou, J. Sun, Y. Chi, X. Cheng, D. Yang, *EcoEnergy* **2024**, 2, 599.
- [30] D. Kundu, B. D. Adams, V. Duffort, S. H. Vajargah, L. F. Nazar, *Nat. Energy* **2016**, 1, 1.
- [31] X. Zhang, J. Zhang, H. Yu, T. L. Madanu, M. Xia, P. Xing, A. Vlad, J. Shu, B. L. Su, *Angew. Chem. Int. Ed.* **2025**, 64, e202414479.
- [32] D. Chen, M. Lu, D. Cai, H. Yang, W. Han, *J. Energy Chem.* **2021**, 54, 712.
- [33] H. Zhang, X. Liu, H. Li, I. Hasa, S. Passerini, *Angew. Chem. Int. Ed.* **2021**, 60, 598.
- [34] N. Zhang, S. Huang, Z. Yuan, J. Zhu, Z. Zhao, Z. Niu, *Angew. Chem. Int. Ed.* **2021**, 60, 2861.
- [35] D. Zhang, L. Miao, Z. Song, X. Zheng, Y. Lv, L. Gan, M. Liu, *Energy Fuels* **2024**, 38, 12510.
- [36] Y. Shuo, Z. Yuwei, Z. Chunyi, *Energy Mater.* **2025**, 5, 500021.
- [37] J. Cao, F. Zhao, W. Guan, X. Yang, Q. Zhao, L. Gao, X. Ren, G. Wu, A. Liu, *Small* **2024**, 20, 2400221.
- [38] Z. Hou, X. Zhang, X. Li, Y. Zhu, J. Liang, Y. Qian, *J. Mater. Chem. A* **2017**, 5, 730.
- [39] J. Shin, J. Lee, Y. Kim, Y. Park, M. Kim, J. W. Choi, *Adv. Energy Mater.* **2021**, 11, 2100676.
- [40] Z. Li, W. Deng, C. Li, W. Wang, Z. Zhou, Y. Li, X. Yuan, J. Hu, M. Zhang, J. Zhu, *J. Mater. Chem. A* **2020**, 8, 17725.
- [41] H. He, H. Qin, J. Wu, X. Chen, R. Huang, F. Shen, Z. Wu, G. Chen, S. Yin, J. Liu, *Energy Storage Mater.* **2021**, 43, 317.
- [42] Y. Ou, Z. Cai, J. Wang, R. Zhan, S. Liu, Z. Lu, Y. Sun, *EcoMat* **2022**, 4, e12167.
- [43] C. Wang, D. Zhang, S. Yue, S. Jia, H. Li, W. Liu, L. Li, *Chem. Rec.* **2024**, 24, e202400142.
- [44] X. Li, F. Ning, L. Luo, J. Wu, Y. Xiang, X. Wu, L. Xiong, X. Peng, *RSC Adv.* **2022**, 12, 8394.
- [45] Z. Chen, T. Liu, Z. Wei, Y. Wang, A. Chen, Z. Huang, D. Cao, N. Li, C. Zhi, *Energy Environ. Sci.* **2025**, 18, 3296.
- [46] G. Lai, J. Lin, W. Mo, X. Li, X. Jin, M. Wu, F. Liu, *J. Am. Chem. Soc.* **2025**, 147, 13071.
- [47] Z. Liu, X. Zhang, Z. Liu, Y. Jiang, D. Wu, Y. Huang, Z. Hu, *Chem. Sci.* **2024**, 15, 7010.
- [48] X. Yang, Q. Zhou, S. Wei, X. Guo, P. J. Chimalti, W. Xu, S. Chen, Y. Cao, P. Zhang, K. Zhu, H. Shou, Y. Wang, X. Wu, C. Wang, L. Song, *Small Methods* **2024**, 8, 2301115.
- [49] W. Cheng, M. Zhao, Y. Lai, X. Wang, H. Liu, P. Xiao, G. Mo, B. Liu, Y. Liu, *Exploration* **2024**, 4, 20230056.

- [50] S. Guo, L. Qin, T. Zhang, M. Zhou, J. Zhou, G. Fang, S. Liang, *Energy Storage Mater.* **2021**, *34*, 545.
- [51] X. Li, J. Miao, F. Hu, K. Yan, L. Song, H. Fan, L. Ma, W. Wang, *J. Mater. Chem. A* **2024**, *12*, 968.
- [52] Z. Liu, R. Wang, Q. Ma, J. Wan, S. Zhang, L. Zhang, H. Li, Q. Luo, J. Wu, T. Zhou, J. Mao, L. Zhang, C. Zhang, Z. Guo, *Adv. Funct. Mater.* **2024**, *34*, 2214538.
- [53] H. Cao, X. Huang, Y. Liu, Q. Hu, Q. Zheng, Y. Huo, F. Xie, J. Zhao, D. Lin, *J. Colloid Interface Sci.* **2022**, *627*, 367.
- [54] K. Guan, L. Tao, R. Yang, H. Zhang, N. Wang, H. Wan, J. Cui, J. Zhang, H. Wang, H. Wang, *Adv. Energy Mater.* **2022**, *12*, 2103557.
- [55] Y. Lin, Z. Mai, H. Liang, Y. Li, G. Yang, C. Wang, *Energy Environ. Sci.* **2023**, *16*, 687.
- [56] L. Tao, K. Guan, R. Yang, Z. Guo, L. Wang, L. Xu, H. Wan, J. Zhang, H. Wang, L. Hu, *Energy Storage Mater.* **2023**, *63*, 102981.
- [57] C. Li, H. Wang, S. Chen, Z. Bai, M. Zhu, H. Wang, D. Chen, Z. Ren, S. Chen, Y. Tang, Y. Zhang, *Small* **2024**, *20*, 2306939.
- [58] C. Jin, C. Yang, L. Xie, H. Mi, H. Yin, B. Xu, F. Guo, J. Qiu, *Adv. Energy Mater.* **2025**, *15*, 2402843.
- [59] Z. Zhang, S. Yan, H. Dong, T. Li, J. Liu, X. Song, E. H. Ang, Q. Wang, Y. Wang, *J. Colloid Interface Sci.* **2025**, *677*, 885.
- [60] Y. Zhang, X. Zheng, K. Wu, Y. Zhang, G. Xu, M. Wu, H.-K. Liu, S.-X. Dou, C. Wu, *Nano Lett.* **2022**, *22*, 8574.
- [61] Q. Yue, Y. Wan, X. Li, Q. Zhao, T. Gao, G. Deng, B. Li, D. Xiao, *Chem. Sci.* **2024**, *15*, 5711.
- [62] K. W. Kim, H. Kim, J. Choi, S.-J. Choi, K. R. Yoon, *Energy Storage Mater.* **2024**, *71*, 103594.
- [63] J. Du, X. Zhan, Y. Xu, D. Zhang, S. Qin, *Nano Lett.* **2024**, *24*, 13592.
- [64] S.-J. Zhang, J. Hao, D. Luo, P.-F. Zhang, B. Zhang, K. Davey, Z. Lin, S.-Z. Qiao, *Adv. Energy Mater.* **2021**, *11*, 2102010.
- [65] H. Li, Y. Gan, X. Chen, J. Wang, T. Ling, B. Shang, W. Li, Q. Li, *Corros. Sci.* **2025**, *246*, 112762.
- [66] C. Wu, C. Sun, K. Ren, F. Yang, Y. Du, X. Gu, Q. Wang, C. Lai, *Chem. Eng. J.* **2023**, *452*, 139465.
- [67] Q. Meng, R. Zhao, P. Cao, Q. Bai, J. Tang, G. Liu, X. Zhou, J. Yang, *Chem. Eng. J.* **2022**, *447*, 137471.
- [68] J. Zhang, X. Wei, Q. Wu, X. Liu, S. Yang, F. Luo, Z. Yan, J. Huang, Y. Chen, *Polym. Sci. Technol.* **2025**
- [69] Y. Zhong, Z. Cheng, H. Zhang, J. Li, D. Liu, Y. Liao, J. Meng, Y. Shen, Y. Huang, *Nano Energy* **2022**, *98*, 107220, <https://doi.org/10.1021/polymscitech.4c00034>.
- [70] W. Liang, D. Li, R. Zhong, S. Tao, Y. Zhu, W. Tan, R. Xu, Y. Yuan, I. Zhitomirsky, J. Lu, *Adv. Funct. Mater.* **2025**, *n/a*, 2504195.
- [71] J. Hao, L. Yuan, Y. Zhu, M. Jaroniec, S.-Z. Qiao, *Adv. Mater.* **2022**, *34*, 2206963.
- [72] L. Miao, Z. Guo, L. Jiao, *Energy Mater.* **2023**, *3*, 300014.
- [73] Y. Xu, X. Li, X. Wang, Q. Weng, W. Sun, *Mater. Today Sustain.* **2024**, *28*, 100948.
- [74] W. Zhou, M. Chen, Y. Quan, J. Ding, H. Cheng, X. Han, J. Chen, B. Liu, S. Shi, X. Xu, *Chem. Eng. J.* **2023**, *457*, 141328.
- [75] P. Luo, D. Li, J. Long, S. Nie, X. Chen, Z. Li, G. Lei, *Chem. Eng. J.* **2024**, *479*, 147727.
- [76] N. Zhang, X. Chen, M. Yu, Z. Niu, F. Cheng, J. Chen, *Chem. Soc. Rev.* **2020**, *49*, 4203.
- [77] N. Li, G. Li, C. Li, H. Yang, G. Qin, X. Sun, F. Li, H.-M. Cheng, *ACS Appl. Mater. Interfaces* **2020**, *12*, 13790.
- [78] W. Huang, H. Wang, R. Hu, J. Liu, L. Yang, M. Zhu, *Small* **2023**, *19*, 2303286.
- [79] Y. Zhang, H. Li, S. Huang, S. Fan, L. Sun, B. Tian, F. Chen, Y. Wang, Y. Shi, H. Y. Yang, *Nano-Micro Lett.* **2020**, *12*, 1.
- [80] V. Soundharrajan, B. Sambandam, S. Kim, S. Islam, J. Jo, S. Kim, V. Mathew, Y.-k. Sun, J. Kim, *Energy Storage Mater.* **2020**, *28*, 407.
- [81] M. Chamoun, W. R. Brant, C.-W. Tai, G. Karlsson, D. Noréus, *Energy Storage Mater.* **2018**, *15*, 351.
- [82] L. Ma, S. Chen, H. Li, Z. Ruan, Z. Tang, Z. Liu, Z. Wang, Y. Huang, Z. Pei, J. A. Zapien, *Energy Environ. Sci.* **2018**, *11*, 2521.
- [83] X. Li, X. Wang, L. Ma, W. Huang, *Adv. Energy Mater.* **2022**, *12*, 2202068.
- [84] X. Zhou, K. Ma, Q. Zhang, G. Yang, C. Wang, *Nano Res.* **2022**, *15*, 8039.
- [85] X. Wang, A. Naveed, T. Zeng, T. Wan, H. Zhang, Y. Zhou, A. Dou, M. Su, Y. Liu, D. Chu, *Chem. Eng. J.* **2022**, *446*, 137090.
- [86] X. Yang, Z. Jia, W. Wu, H.-Y. Shi, Z. Lin, C. Li, X.-X. Liu, X. Sun, *Chem. Commun.* **2022**, *58*, 4845.
- [87] X. Guo, Z. Zhang, J. Li, N. Luo, G.-L. Chai, T. S. Miller, F. Lai, P. Shearing, D. J. L. Brett, D. Han, Z. Weng, G. He, I. P. Parkin, *ACS Energy Lett.* **2021**, *6*, 395.
- [88] Z. Hu, F. Zhang, Y. Zhao, H. Wang, Y. Huang, F. Wu, R. Chen, L. Li, *Adv. Mater.* **2022**, *34*, 2203104.
- [89] M. Wang, Y. Meng, X. Li, J. Qi, A. Li, S. Huang, *Chem. Eng. J.* **2025**, *507*, 160615.
- [90] B. B. Upreti, N. Kamboj, R. S. Dey, *Small* **2025**, *21*, 2408138.
- [91] Z. Zeng, Y. Zeng, L. Sun, H. Mi, L. Deng, P. Zhang, X. Ren, Y. Li, *Nanoscale* **2021**, *13*, 12223.
- [92] A. R. Mainar, E. Iruin, L. C. Colmenares, J. A. Blázquez, H.-J. Grande, *Energy Sci. Eng.* **2018**, *6*, 174.
- [93] Y. Ma, J. Huang, S. Gao, L. Li, Z. Yi, D. Xiao, C. K. K. Chan, B. Wang, D. Pan, Q. Chen, *Angew. Chem. Int. Ed* **2025**, *64*, e202425261.
- [94] W. Liu, M. Chen, D. Ren, J. Tang, J. Sun, X. Zhang, B. Jiang, F. Jiang, F. Kang, *J. Colloid Interface Sci.* **2024**, *657*, 931.
- [95] W. Zhang, Y. Dai, R. Chen, Z. Xu, J. Li, W. Zong, H. Li, Z. Li, Z. Zhang, J. Zhu, F. Guo, X. Gao, Z. Du, J. Chen, T. Wang, G. He, I. P. Parkin, *Angew. Chem. Int. Ed* **2023**, *62*, e202212695.
- [96] S. Bai, Z. Huang, G. Liang, R. Yang, D. Liu, W. Wen, X. Jin, C. Zhi, X. Wang, *Adv. Sci.* **2024**, *11*, 2304549.
- [97] B. Hu, Y. Wang, X. Qian, W. Chen, G. Liang, J. Chen, J. Zhao, W. Li, T. Chen, J. Fu, *ACS Nano* **2023**, *17*, 12734.
- [98] N. A. Thieu, W. Li, X. Chen, Q. Li, Q. Wang, M. Velayutham, Z. M. Grady, X. Li, W. Li, V. V. Khamrakov, D. M. Reed, X. Li, X. Liu, *ACS Appl. Mater. Interfaces* **2023**, *15*, 55570.
- [99] K. Wang, M. Qin, C. Wang, T. Yan, Y. Zhen, X. Sun, J. Wang, F. Fu, *J. Colloid Interface Sci.* **2023**, *629*, 733.
- [100] P. Xue, C. Guo, N. Wang, K. Zhu, S. Jing, S. Kong, X. Zhang, L. Li, H. Li, Y. Feng, W. Gong, Q. Li, *Adv. Funct. Mater.* **2021**, *31*, 2106417.
- [101] M. A. Zabara, B. Y. Kaplan, S. A. Gürsel, A. Yürüm, *Adv. Mater. Interfaces* **2023**, *10*, 2300555.
- [102] N. Naresh, S. Eom, S. H. Jeong, S. J. Lee, S. H. Park, J. Park, J.-H. Ahn, J.-H. Kim, Y. H. Jung, *Appl. Surf. Sci.* **2022**, *606*, 154932.
- [103] Y. Chen, H. Ding, S. Sun, *Nanomaterials* **2017**, *7*, 217.
- [104] D. Guo, F. Li, B. Zhang, *Adv. Sci.* **2025**, *12*, 2411995.
- [105] Q. Shen, Y. Wang, G. Han, X. Li, T. Yuan, H. Sun, Y. Gong, T. Chen, *Batteries* **2023**, *9*, 284.
- [106] D. Li, L. Cao, T. Deng, S. Liu, C. Wang, *Angew. Chem. Int. Ed* **2021**, *60*, 13035.
- [107] X. Chen, C. Liu, X. Bai, J. Zhang, X. Chang, L. Hou, H. Huang, Y. Wei, B. Wu, W. Liu, Q. Wang, *Energy Storage Mater.* **2025**, *75*, 103984.
- [108] H. J. Kim, S. Kim, K. Heo, J.-H. Lim, H. Yashiro, S.-T. Myung, *Adv. Energy Mater.* **2023**, *13*, 2203189.
- [109] J. Shin, J. Lee, Y. Park, J. W. Choi, *Chem. Sci.* **2020**, *11*, 2028.
- [110] W. Yuan, G. Ma, X. Nie, Y. Wang, S. Di, L. Wang, J. Wang, S. Shen, N. Zhang, *Chem. Eng. J.* **2022**, *431*, 134076.
- [111] L. Yu, J. Huang, S. Wang, L. Qi, S. Wang, C. Chen, *Adv. Mater.* **2023**, *35*, 2210789.
- [112] J. Chen, W. Zhou, Y. Quan, B. Liu, M. Yang, M. Chen, X. Han, X. Xu, P. Zhang, S. Shi, *Energy Storage Mater.* **2022**, *53*, 629.
- [113] M. Zhong, Y. Wang, Y. Xie, S. Yuan, K. Ding, E. J. Begin, Y. Zhang, J. L. Bao, Y. Wang, *Adv. Funct. Mater.* **2024**, *34*, 2316788.
- [114] J. Cao, Y. Sun, D. Zhang, D. Luo, H. Wu, X. Wang, C. Yang, L. Zhang, X. Yang, J. Qin, *ChemElectroChem* **2024**, *11*, e202400064.
- [115] J. Pereira, R. Souza, A. Moreira, A. Moita, *Ionics* **2024**, *30*, 4343.
- [116] J. Pereira, R. Souza, A. Moreira, A. Moita, *Inorganics* **2024**, *12*, 186.
- [117] S. Zafar, M. Sharma, S. N. Mahapatra, B. Lochab, *Chem. Commun.* **2025**, *61*, 3151.
- [118] X. Ma, X. Cao, M. Yao, L. Shan, X. Shi, G. Fang, A. Pan, B. Lu, J. Zhou, S. Liang, *Adv. Mater.* **2022**, *34*, 2105452.
- [119] W. Zhang, Y. Lv, W. Xiong, L. Gan, M. Liu, *Batteries Supercaps* **2025**, *8*, e202400507.
- [120] M. I. Ahmad, D. Bahtiyar, H. W. Khan, M. U. H. Shah, L. Kiran, M. K. Aydinol, M. Yusuf, H. Kamyab, S. Rezania, *J. Energy Storage* **2023**, *72*, 108765.
- [121] M. Yang, X. Zou, M. Wu, J. Yu, X. Ma, Y. Hu, F. Yan, *Energy Environ. Sci.* **2025**, *18*, 3365.
- [122] C. Poochai, T. Kongthong, J. Lohitkarn, N. Maeboonruan, S. Pothaya, R. Checharoen, C. Srirachabuwong, *Diamond Relat. Mater.* **2025**, *154*, 112095.
- [123] C. Shen, Y. Zhang, X. Li, P. Guo, X. Zeng, K. Ni, R. Cao, Z. Wang, Z. Wang, L. Qin, *J. Mater. Chem. A* **2025**, *13*, 2174.
- [124] N. Zhang, F. Cheng, J. Liu, L. Wang, X. Long, X. Liu, F. Li, J. Chen, *Nat. Commun.* **2017**, *8*, 405.
- [125] L. Suo, O. Borodin, T. Gao, M. Olguin, J. Ho, X. Fan, C. Luo, C. Wang, K. Xu, *Science* **2015**, *350*, 938.

- [126] C. Nie, G. Wang, D. Wang, M. Wang, X. Gao, Z. Bai, N. Wang, J. Yang, Z. Xing, S. Dou, *Adv. Energy Mater.* **2023**, *13*, 2300606.
- [127] G. Li, L. Sun, S. Zhang, C. Zhang, H. Jin, K. Davey, G. Liang, S. Liu, J. Mao, Z. Guo, *Adv. Funct. Mater.* **2024**, *34*, 2301291.
- [128] H. Yan, X. Zhang, Z. Yang, M. Xia, C. Xu, Y. Liu, H. Yu, L. Zhang, J. Shu, *Coord. Chem. Rev.* **2022**, *452*, 214297.
- [129] F. Zhao, Z. Jing, X. Guo, J. Li, H. Dong, Y. Tan, L. Liu, Y. Zhou, R. Owen, P. R. Shearing, *Energy Storage Mater.* **2022**, *53*, 638.
- [130] B. Wu, T. Lu, X. Bai, J. Zhang, X. Chang, L. Hou, Y. Wei, Q. Wang, J. Ni, *Small Methods* **2025**, *n/a*, 2401838.
- [131] F. Jing, L. Xu, Y. Shang, G. Chen, C. Lv, C. Yan, *J. Colloid Interface Sci.* **2024**, *669*, 984.
- [132] L. Cao, D. Li, E. Hu, J. Xu, T. Deng, L. Ma, Y. Wang, X.-Q. Yang, C. Wang, *J. Am. Chem. Soc.* **2020**, *142*, 21404.
- [133] Y. Zhu, J. Hao, Y. Huang, Y. Jiao, *Small Struct.* **2023**, *4*, 2200270.
- [134] Y. Zhu, Q. Chen, J. Hao, Y. Jiao, *J. Mater. Chem. A* **2024**, *12*, 20097.
- [135] R. Meng, H. Li, Z. Lu, C. Zhang, Z. Wang, Y. Liu, W. Wang, G. Ling, F. Kang, Q.-H. Yang, *Adv. Mater.* **2022**, *34*, 2200677.
- [136] N. Wang, S. Zhai, Y. Ma, X. Tan, K. Jiang, W. Zhong, W. Zhang, N. Chen, W. Chen, S. Li, G. Han, Z. Li, *Energy Storage Mater.* **2021**, *43*, 585.
- [137] P. Sun, L. Ma, W. Zhou, M. Qiu, Z. Wang, D. Chao, W. Mai, *Angew. Chem.* **2021**, *133*, 18395.
- [138] R. Zhao, H. Wang, H. Du, Y. Yang, Z. Gao, L. Qie, Y. Huang, *Nat. Commun.* **2022**, *13*, 3252.
- [139] M. He, C. Shu, A. Hu, R. Zheng, M. Li, Z. Ran, J. Long, *Energy Storage Mater.* **2022**, *44*, 452.
- [140] W. Xu, K. Zhao, W. Huo, Y. Wang, G. Yao, X. Gu, H. Cheng, L. Mai, C. Hu, X. Wang, *Nano Energy* **2019**, *62*, 275.
- [141] J. Wang, Y. Yang, Y. Zhang, Y. Li, R. Sun, Z. Wang, H. Wang, *Energy Storage Mater.* **2021**, *35*, 19.
- [142] W. Lu, C. Xie, H. Zhang, X. Li, *ChemSusChem* **2018**, *11*, 3996.
- [143] J. Cao, D. Zhang, C. Gu, X. Wang, S. Wang, X. Zhang, J. Qin, Z.-S. Wu, *Adv. Energy Mater.* **2021**, *11*, 2101299.
- [144] T. Wang, Q. Xi, Y. Li, H. Fu, Y. Hua, E. G. Shankar, A. K. Kakarla, J. S. Yu, *Adv. Sci.* **2022**, *9*, 2200155.
- [145] Z. Song, C. Yang, N. Kiatwisarnkij, A. Lu, N. Tunghathaithip, K. Lolupiman, T. Bovornratanarak, X. Zhang, G. He, J. Qin, *ACS Appl. Mater. Interfaces* **2024**, *16*, 64834.
- [146] G. Lin, X. Zhou, L. Liu, D. Huang, H. Li, X. Cui, J. Liu, *RSC Adv.* **2022**, *12*, 25054.
- [147] H. Yin, H. Wu, Y. Yang, S. Yao, P. Han, Y. Shi, R. Liu, *Small* **2024**, *20*, 2404367.
- [148] H. Zhang, Y. Zhong, J. Li, Y. Liao, J. Zeng, Y. Shen, L. Yuan, Z. Li, Y. Huang, *Adv. Energy Mater.* **2023**, *13*, 2203254.
- [149] C. Zhai, D. Zhao, Y. He, H. Huang, B. Chen, X. Wang, Z. Guo, *Batteries* **2022**, *8*, 153.
- [150] P. Wang, X. Xie, Z. Xing, X. Chen, G. Fang, B. Lu, J. Zhou, S. Liang, H. J. Fan, *Adv. Energy Mater.* **2021**, *11*, 2101158.
- [151] M. Qiu, P. Sun, Y. Wang, L. Ma, C. Zhi, W. Mai, *Angew. Chem. Int. Ed.* **2022**, *61*, e202210979.
- [152] Q. Wu, J. Huang, J. Zhang, S. Yang, Y. Li, F. Luo, Y. You, Y. Li, H. Xie, Y. Chen, *Angew. Chem. Int. Ed.* **2024**, *63*, e202319051.
- [153] P. Sun, L. Ma, W. Zhou, M. Qiu, Z. Wang, D. Chao, W. Mai, *Angew. Chem. Int. Ed.* **2021**, *60*, 18247.
- [154] B. Liu, L. Yu, Q. Xiao, S. Zhang, G. Li, K. Ren, Y. Zhu, C. Wang, Q. Wang, *Chem. Sci.* **2024**, *15*, 16118.
- [155] F. Xiao, X. Wang, K. Sun, Q. Zhao, C. Han, H.-F. Li, *Chem. Eng. J.* **2024**, *489*, 151111.
- [156] J. Leng, X. Wang, D. Li, R. Shi, X. Zhu, L. Cao, Q. An, *J. Energy Storage* **2025**, *121*, 116502.
- [157] S. Liu, J. Mao, W. K. Pang, J. Vongsivut, X. Zeng, L. Thomsen, Y. Wang, J. Liu, D. Li, Z. Guo, *Adv. Funct. Mater.* **2021**, *31*, 2104281.
- [158] Y. Xie, S. Feng, J. Gao, T. Cheng, L. Zhang, *Sci. China Mater.* **2024**, *67*, 2898.
- [159] Y. Shang, V. Kundu, I. Pal, H. N. Kim, H. Zhong, P. Kumar, D. Kundu, *Adv. Mater.* **2024**, *36*, 2309212.
- [160] L. Li, Y. Xie, M. Yao, R. Cao, X. Mai, Y. Ji, L. Chen, X. Dong, Y. Xia, *Chem. Commun.* **2024**, *60*, 6809.
- [161] Z. Cao, X. Ma, W. Liu, J. Wu, Y. Jiao, Y. Yin, Z. Lu, S. Yang, *Adv. Funct. Mater.* **2025**, *35*, 2414956.
- [162] G. Zhang, Y. Chen, L. Fu, L. Zheng, K. Fan, C. Zhang, J. Zou, H. Dai, L. Guan, Y. Cao, M. Mao, J. Ma, C. Wang, *SmartMat* **2024**, *5*, e1216.
- [163] B. Tang, L. Shan, S. Liang, J. Zhou, *Energy Environ. Sci.* **2019**, *12*, 3288.
- [164] Z. Yang, Y. Sun, S. Deng, H. Tong, M. Wu, X. Nie, Y. Su, G. He, Y. Zhang, J. Li, *Energy Environ. Sci.* **2024**, *17*, 3443.
- [165] X. Han, J. Han, K. Ma, J. Wen, L. Li, D. Han, J. Sun, *Energy Environ. Sci.* **2024**, *17*, 9244.
- [166] S. Zhao, C. Li, X. Zhang, N. Li, T. Wang, X. Li, C. Wang, G. Qu, X. Xu, *Sci. Bull.* **2023**, *68*, 56.
- [167] X. Hu, F. Gao, Y. Xiao, D. Wang, Z. Gao, Z. Huang, S. Ren, N. Jiang, S. Wu, *Chem. Eng. J.* **2024**, *481*, 148450.
- [168] Y. Wang, Z. Wu, F. M. Azad, Y. Zhu, L. Wang, C. J. Hawker, A. K. Whittaker, M. Forsyth, C. Zhang, *Nat. Rev. Mater.* **2024**, *9*, 119.
- [169] P. T. Bhutia, S. Grugeon, A. E. Mejdoubi, S. Laruelle, G. Marlair, *Batteries* **2024**, *10*, 370.
- [170] S. Yang, L. Mei, Z. Wu, J. Zhu, P. Li, H. Hong, Z. Zeng, H. Li, F. Mo, C. Zhi, *Energy Environ. Sci.* **2024**, *17*, 7424.
- [171] R. Wang, Q. Ma, L. Zhang, Z. Liu, J. Wan, J. Mao, H. Li, S. Zhang, J. Hao, L. Zhang, C. Zhang, *Adv. Energy Mater.* **2023**, *13*, 2302543.
- [172] L. Zhang, Y. Han, Y. Geng, H. Zhang, H. Liu, Y. He, Z. Yan, Z. Zhu, *Angew. Chem. Int. Ed.* **2025**, *64*, e202500434.

Manuscript received: May 30, 2025

Revised manuscript received: July 16, 2025

Version of record online: